JOURNAL OF GEOPHYSICAL RESEARCH, VOL. 105, NO. D3, PAGES 3605–3631, FEBRUARY 16, 2000

Pollution from aircraft emissions in the North Atlantic flight corridor: Overview on the POLINAT projects

U. Schumann,[1] H. Schlager,[1] F. Arnold,[2] J. Ovarlez,[3] H. Kelder,[4,5] Ø. Hov,[6] G. Hayman,[7] I. S. A. Isaksen,[8] J. Staehelin,[9] and P. D. Whitefield[10]

Abstract. The Pollution From Aircraft Emissions in the North Atlantic Flight Corridor (POLINAT) projects were undertaken to investigate the impact of aircraft engine exhaust emissions on the state of the atmosphere in the North Atlantic flight corridor. Changes in the composition of the lower stratosphere and upper troposphere from aircraft emissions are identified from combined measurements and model analyses. Measurements were performed using the Deutsches Zentrum für Luft- und Raumfahrt Falcon research aircraft and a Swissair B-747 over the North Atlantic covering the altitude range 6 to 13 km in November 1994 and June/July 1995 and from August to November 1997. The measurements include those of nitrogen oxides, nitrous and nitric acids, sulfur dioxide, sulfuric acid, acetone, carbon dioxide, ozone, water vapor, carbon monoxide, aerosols, and meteorological parameters. The atmospheric composition was found to be highly variable, and emissions from sources at the surface or from lightning discharges also contribute strongly to the nitrogen oxides abundance and ozone formation. Contributions from aircraft emissions have been measured and identified in single and multiple plumes of several hours ages, and accumulation of such nitrogen oxides and particles emissions can be identified under certain conditions in and downstream of the flight corridor region. Acetone was found at high mixing ratios. The global and regional models predict ozone increases of 3 to 6% by current air traffic at the flight corridor altitude north of 30°N, in agreement with previous model analyses but too small to be measurable. In autumn, the upper troposphere is often humid with water vapor concentration far above ice saturation, providing conditions for persistent contrails.

1. Introduction

Aircraft cruising near the tropopause may cause significant changes in the atmospheric composition, chemistry, and cloud formation with potential consequences for the ozone concentration in parts of the upper troposphere and lower stratosphere and for the climate of the Earth's atmosphere [*Schumann*, 1994]. Aircraft engines emit nitrogen oxides (NO_x, the sum of nitric oxide, NO, and nitrogen dioxide, NO_2), particles, particle precursor gases, and other species. Because of high air traffic density remote from other sources, the effect of aircraft emissions is expected to be measurable within the North Atlantic flight corridor (NAFC). Very few data were available before 1994 in the altitude range of cruising subsonic jet airliners (up to 13 km), and no data were available within the NAFC. Therefore the project "Pollution From Aircraft Emissions in the North Atlantic Flight Corridor" was performed in two phases from 1994 to 1998 (POLINAT 1 and 2). This paper gives an overview of the objectives, methods, and accomplishments of both project phases. Further results are described in other papers of the special section in this journal and in a special Subsonic Assessment Ozone and Nitrogen Oxide Experiment (SONEX)/POLINAT issue of the *Geophysical Research Letters* [*Singh et al.*, 1999; *Schlager et al.*, 1999].

The emissions of subsonic aviation and its impact on the state of the atmosphere have been investigated in a sequence of research programs since the early 1990s [*Schumann*, 1994; *World Meteorological Organization (WMO)*, 1995; *Friedl*, 1997; *Brasseur et al.*, 1998; *International Panel on Climate Change (IPCC)*, 1999]. As the first in a sequence of European projects on this topic, the AERONOX project was performed from 1992 to 1994 [*Schumann*, 1995, 1997a]. Model studies within that project predicted large aircraft contributions (20 to 70%, depending on season) to the concentrations of nitrogen oxides in the upper troposphere at 30°-60°N [*Köhler et al.*, 1997; *van Velthoven et al.*, 1997]. Three-dimensional (3-D)

[1]Institut für Physik der Atmosphäre, Deutsches Zentrum für Luft- und Raumfahrt, Oberpfaffenhofen, Germany.
[2]Bereich Atmosphärenphysik, Max-Planck-Institut für Kernphysik, Heidelberg, Germany.
[3]Laboratoire de Météorologie Dynamique du CNRS, Palaiseau, France.
[4]Koninklijk Nederlands Meteorologisch Instituut, AE de Bilt, Netherlands.
[5]Also at the Centre for Theoretical Physics at Technical University Eindhoven, Netherlands.
[6]Norsk Institutt for Luftforskning, Lillestrom, Norway.
[7]National Environmental Technology Centre, AEA Technology, Culham, Abingdon, England, U.K.
[8]Department of Geophysics, University of Oslo, Oslo, Norway.
[9]Institute for Atmospheric Science, Eidgenössische Technische Hochschule, Zürich, Switzerland.
[10]Laboratory for Cloud and Aerosol Science, University of Missouri-Rolla, Rolla.

Paper number 1999JD900941.
0148-0227/00/1999JD900941$09.00

global [*Berntsen and Isaksen*, 1997; *Wauben et al.*, 1997a; *Stevenson et al.*, 1997] and regional [*Flatøy and Hov*, 1996; *Hov and Flatøy*, 1997] chemical transport models (CTM) predicted photochemical ozone generation at time scales of months and of the order of 4 to 10% of background concentrations in the upper troposphere due to present NO_x aircraft emissions. At the same time, similar model studies [*Brasseur et al.*, 1996, 1998; *Friedl*, 1997] concluded somewhat smaller impact of aircraft emissions on nitrogen oxide and ozone abundances, mainly because of smaller emission amounts and different estimates of background concentrations. Also, the local conversion of emitted NO_x in the exhaust plumes into nitric acid reduces the amount of large-scale ozone generation [*Meijer et al.*, 1997]. Increased ozone near the tropopause is expected to enhance the radiative forcing of the atmosphere and to have an impact on the Earth's climate [*Hauglustaine et al.*, 1994; *Sausen et al.*, 1997]. Recently, it was noted that aircraft NO_x may cause a larger reduction of methane than expected from earlier two-dimensional model studies, counterbalancing a significant part of the climate forcing by the induced ozone [*Fuglestvedt et al.*, 1996, 1999; *Isaksen and Jackman*, 1999]. Future nitrogen oxides and ozone changes in the atmosphere due to growing aircraft NO_x emissions are slightly mitigated by an enhanced hydrological cycle in the future climate [*Grewe et al.*, 1999].

Some of the differences in previous estimates of the amounts of NO_x emissions from aircraft [*Lee et al.*, 1997] were due to different values of the assumed emission indices (emission mass per burnt fuel mass). The previous emission databases were derived using surface based measurements and corrections for the effects of altitude. The emissions in the first set of published databases differed by up to a factor of 2 [*Baughcum et al.*, 1993; *Gardner et al.*, 1997]. At the beginning of this project no data were available to validate the assumed emission indices, in particular for wide-body aircraft which cause the largest fraction of the aircraft emissions at cruise altitudes. For instance, *Gardner et al.* [1997] estimated that B-747 aircraft with JT9D engines caused about 33% of all subsonic NO_x emissions, while the same aircraft/engine combination caused 2.8 times smaller emission amounts in the estimate of *Baughcum et al.* [1993].

Previous model estimates often assumed rather low background NO_x concentrations, in particular in summer, often less than 50 pptv (1 pptv = 1 parts per trillion by volume = 1 pmol mol^{-1}), and predicted C-shaped profiles with minima in the midtroposphere and strong increases in the boundary layer over polluted regions and increases above the tropopause because of higher NO_x-lifetime and stratospheric sources [*Drummond et al.*, 1988; *Penner et al.*, 1991; *Ehhalt et al.*, 1992; *WMO*, 1995; *Hauglustaine et al.*, 1998]. Very few NO data were available to check these computations in the North Atlantic region from measurements [*Weinheimer et al.*, 1994; *Emmons et al.*, 1997; *Rohrer et al.*, 1997a; *Thakur et al.*, 1999; *Ziereis et al.*, 1999a]. The models used rather coarse resolution causing intrinsic smoothing of the concentration change caused by the local emissions of individual aircraft. *Schumann and Konopka* [1994] noted that the time required for dispersion of exhaust plumes from aircraft to the outer scale of the corridor or to the level of background concentrations is large compared to the daily period of aircraft emissions leading to a "peaky" concentration field which is inhomogeneous with many large and narrow concentration peaks over a low, relatively smooth background level. Models predict a strong seasonal cycle of the NO_x burden in the upper troposphere [e.g., *Köhler et al.*, 1997; *Hauglustaine et al.*, 1998]. NO data were obtained earlier along the northern edge of the NAFC between Prestwick (56°N, 9°W), Keflavik (Iceland), Sondrestrom (Greenland), and Goose Bay (53°N, 60°W) at up to 12 km altitude during one flight in June 1984 and one in January 1991 [*Drummond et al.*, 1988; *Rohrer* al., 1997a]. The measurements provided snapshots of the highly variable NO concentration. NO_2 was not measured on these occasions. The first measurements of aircraft emissions in subsonic aircraft plumes and in the NAFC were performed within the German research project "Pollutants from Air Traffic" ("Schadstoffe in der Luftfahrt") [*Arnold et al.*, 1992; *Schumann et al.*, 1995; *Schulte and Schlager*, 1996; *Rohrer et al.*, 1997b; *Klemm et al.*, 1998; *Slemr et al.*, 1998; *Ziereis et al.*, 1999a]. Systematic NO_x measurements were made from May 1995 to May 1996 within the Swiss Nitrogen Oxides and Ozone along Air Routes (NOXAR) project [*Brunner et al.*, 1998; *Dias-Lalcaca et al.*, 1998]. The results from these projects provided the basis for the POLINAT projects. POLINAT 1 was the first project that offered the potential to verify the relatively large calculated NO_x impact from subsonic aircraft on the NO_x concentration in a main air traffic corridor near the tropopause at midlatitudes [*Schlager et al.*, 1996].

The impact of aircraft emissions on ozone depends on the background of ozone, carbon monoxide, and water vapor concentrations, the rate of conversion of NO_x to nitric acid (HNO_3) and the total reactive nitrogen gases, collectively called NO_y, and on hydroxyl radicals (HO_x) [*Ehhalt and Rohrer*, 1994; *Flatøy and Hov*, 1996; *Brasseur et al.*, 1996; *Grooß et al.*, 1998]. Ozone and water vapor climatologies over the North Atlantic have recently become available from the MOZAIC project [*Marenco et al.*, 1998]. A set of NO_y data were reported by *Klemm et al.* [1998]. NO_y data outside the corridor in the North Atlantic region were measured during the STREAM project [*Schneider et al.*, 1998]. An important HO_2 formation process which does not consume O_3 in the upper troposphere involves acetone [*Singh et al.*, 1995; *Arnold et al.* 1997a, b; *Wennberg et al.*, 1998; *Hauglustaine et al.*, 1998]. Acetone enhances O_3 formation due to aircraft NO_x emissions [*Müller and Brasseur*, 1999]. Despite its early detection in the upper troposphere by *Hauck and Arnold* [1984], measurements of acetone are still limited to those of *Arnold et al.* [1997a, b] over the North Atlantic and of *Singh et al.* [1995, 1998] mostly over the Pacific.

Aircraft engines also emit particles and cause aerosol trails [*Fahey et al.*, 1995; *Hagen et al.*, 1996; *Schumann et al.*, 1996]. In sufficiently cold air, water vapor emissions cause contrails with properties depending on the induced particles [*Kärcher et al.*, 1998]. Models predict a small climate response for present contrail coverage estimates [*Ponater et al.*, 1996; *IPCC*, 1999]. Contrail particles may grow and persist for hours in ice supersaturated air masses [*Schumann*, 1996; *Heymsfield et al.*, 1998; *Jensen et al.*, 1998]. Therefore climatological water vapor data as provided by MOZAIC are of high importance. Because of the difficulties in performing automatic, routine humidity measurements with high accuracy on airliners [*Helten et al.*, 1998], we saw a need for in situ validation of the MOZAIC measurements.

The POLINAT projects were initiated in 1993 and performed in two phases. The first phase, POLINAT 1, was per-

formed from January 1994 to August 1996 within the Environment Research Program of the European Commission [*Schumann*, 1997b]. The second phase, POLINAT 2, was performed from April 1996 to September 1998 within the Environment and Climate Research Program of the European Commission [*Schumann*, 1999]. The objectives of the POLINAT projects were threefold: (1) to determine the composition, spatial and temporal distribution, and transformation of pollutants emitted from jet engines of subsonic aircraft at cruise altitudes near the tropopause within a flight corridor with heavy air traffic, (2) to determine by measurements and analyses the relative contributions from air traffic exhaust emissions to the composition of the atmosphere in and near the flight corridor, and (3) to assess the effects of air traffic emissions in that region in relation to background concentrations and pollutant contributions from other sources and to analyze their importance for changes in ozone, oxidizing capacity, aerosols, and cloud formation. The POLINAT 1 project concentrated on the objective 1 and provided preliminary results on objective 3. The POLINAT 2 project focused on the objectives 2 and 3. In particular, the latter project addressed the following questions: (1) What is the mean abundance of aircraft emitted species and other related species vertically and horizontally across and along the corridor? (2) What are the effective emissions, dispersion, chemical conversion, and particle formation in single and multiple plumes from one or several aircraft? (3) At what time scales and space scales do the pollutants become homogeneously mixed? (4) Is there a measurable large-scale impact of aircraft emissions on the composition of the tropopause region? (5) What are the contributions from air traffic sources in relation to surface emissions? (6) How frequent is air at flight levels supersaturated with respect to the ice phase? (7) How do the instruments perform in flight in comparison to other instruments? (8) How do the models perform in comparison to observations? (9) What are the consequences of the aircraft emissions of nitrogen oxides and other trace substances on the formation of ozone and other chemicals in the troposphere and lower stratosphere? and (10) What can be learned about atmospheric dynamics from the measurements and model results?

The projects were performed by partners from seven European and one American organizations: DLR, MPI-K, LMD, KNMI, AEA, NILU, ETH, and UMR (see Table 1 for explanation of the abbreviations), in formal cooperation with further European partners: UK Meteorological Office, UCL, UO, and UB, with support from the European Commission. Part of the measurements were performed by DLR and MPI-K in cooperation with FhG-IFU and supported within the German national research program "Pollutants from Air Traffic" [*Schumann et al.*, 1997].

The POLINAT projects were coordinated with several other European and American projects. In particular, the POLINAT 2 aircraft campaign was closely coordinated with the NASA research program SONEX [*Singh et al.*, 1999]. During SONEX, an instrumented DC-8 aircraft also performed measurements in the North Atlantic region from October to November 1997. These measurements complement the results obtained within POLINAT 2 with the Falcon and the B-747. Moreover, some measurements of the POLINAT team were coordinated with the Atmospheric Chemistry Studies in the Oceanic Environment (ACSOE), North Atlantic Regional Experiment (NARE), and Measurement of Ozone by Airbus in-service Aircraft (MOZAIC [*Marenco et al.*, 1998]) projects. POLINAT 1 and 2 contained two major tasks: Measurements and modeling. The model activities were performed in close cooperation with the project Modeling of the Impact of Aircraft Emissions on Ozone and other Chemical Components of the Atmosphere (AEROCHEM). Subsequently, first the measurements and modeling activities are described, and then the major results are summarized.

Table 1. Acronyms

	Definitions
ACSOE	Atmospheric Chemistry Studies in the Oceanic Environment
AEA	AEA Technology, National Environmental Technology Centre, Culham, Abingdon, U.K.
AEROCHEM	Modeling of the Impact of Aircraft Emissions on Ozone and Other Chemical Components of the Atmosphere
AERONOX	The Impact of NO_x Emissions From Aircraft Upon the Atmosphere at Flight Altitudes 8-15 km
CN	Condensation Nuclei
CTM	Chemical Transport Model
DERA	DERA, Propulsion Department, Pyestock, Hampshire, U.K.
DLR	Deutsches Zentrum für Luft- und Raumfahrt (German Aerospace Center), Oberpfaffenhofen
ECMWF	European Centre for Medium-Range Weather Forecasts
EI	Emission Index (mass or number of exhaust species per mass of fuel burnt)
ETH	Eidgenössische Technische Hochschule, Institute for Atmospheric Science, Zürich, Switzerland
FhG-IFU	Fraunhofer Gesellschaft, Institut für Atmosphärische Umweltforschung, Garmisch, Germany
ICAO	International Civil Aviation Organization, Montreal and Paris
KNMI	Koninklijk Nederlands Meteorologisch Instituut, AE de Bilt, Netherlands
LMD	Laboratoire de Météorologie Dynamique du CNRS, Palaiseau, France
MOZAIC	Measurement of Ozone by Airbus In-Service Aircraft
MPI-K	Max-Planck-Institut für Kernphysik, Atmospheric Physics Division, Heidelberg, Germany
MRF	Meteorological Research Flight of U.K. Meteorological Office
NAFC	North Atlantic Flight Corridor
NARE	North Atlantic Regional Experiment
NASA	National Aeronautics and Space Administration
NILU	Norsk institutt for luftforskning, Lillestrom, Norway
NOXAR	Nitrogen Oxides and Ozone along Air Routes
OTS	Organized Track System
POLINAT	Pollution From Aircraft Emissions in the North Atlantic Flight Corridor
PVU	Potential Vorticity Unit, 10^{-6} K m^2 kg^{-1} s^{-1}
RH	relative humidity with respect to liquid water saturation
SONEX	Subsonic Assessment Ozone and Nitrogen Oxides Experiment
STREAM	Stratosphere-Troposphere Experiments by Aircraft Measurements
UB	University of Bergen, Norway
UCL	University College London, Department of Physics and Astronomy, London, U.K.
UK Met. Office	Meteorological Office, Bracknell, U.K.
UMR	University of Missouri-Rolla, Rolla, Missouri, United States of America
UO	University of Oslo, Norway
1-D, 2-D, 3-D	one-, two-, three-dimensional

2. POLINAT Measurements

2.1. Selection of the Experimental Region: the North Atlantic Flight Corridor

The NAFC was selected as experimental area because it is an area with strong impact from aircraft emissions while other sources are remote with less direct impact [*Schumann*, 1994]. Depending on season, about 30 to 70% of traffic in the NAFC occurs in the lower stratosphere [*Hoinka et al.*, 1993]. Annual traffic statistics are compiled by the International Civil Aviation Organization (ICAO) with further details for the weeks of July 1-7 and November 1-7 each year, see Table 2 [*ICAO*, 1997; *Ker*, 1998]. The annual mean number of aircraft movements passing the North Atlantic in both directions per day has increased from 390 in 1986 to more than 800 in 1997 and may exceed 1300 in 2015, see Figure 1 [*ICAO*, 1997]. The most popular route is between central Europe and the eastern part of North America (Table 2). The traffic peaks in July (31% above average), is a little lower in November (10% above average), and lowest in February. About 70% of all traffic over the North Atlantic passes 30°W between 45°N and 65°N. Half of the westbound traffic passes 30°W between 12 and 16 UTC with busiest hours between 14 and 15 UTC in summer on Friday; half of the eastbound traffic passes 30°W between 2 and 5 UTC and peaks between 4 and 5 UTC on Sunday [*Ker*, 1998]. About 50% of all the aircraft flying over the North Atlantic are four- or three-engine wide body aircraft. The remaining fraction consists of twin-engined aircraft and this fraction is increasing. The fraction of supersonic transport is of the order of 1% and decreasing.

During the POLINAT 2 project, as shown in Figure 2, most traffic passed the Shannon air traffic control zone between flight levels from 9.4 km (310 hft) to 11.3 km (370 hft; flight levels are usually measured in hectofeet, 1 hft = 100 ft = 30.48 m), that is, at pressure levels from 290 to 200 hPa, with maximum traffic of about 90 aircraft per day at flight levels 310 and 370 hft, westbound and eastbound, respectively. A very small number of supersonic aircraft passed the NAFC near flight level 18.3 km (600 hft).

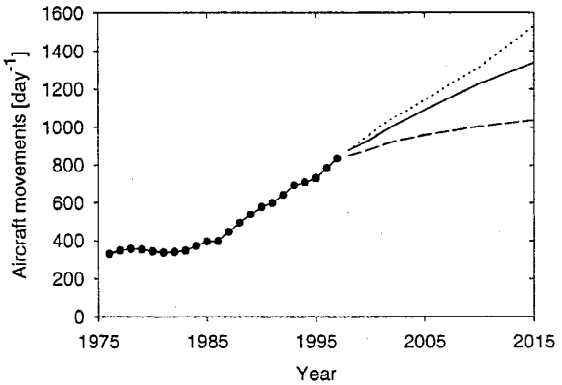

Figure 1. Number of aircraft movements across the North Atlantic per day over the years 1976 to 1997 and forecasts for the future. Full curve with circles: past annual mean traffic, full curve: best estimate forecast, long- and short-dashed: high and low forecast limits. Data from *ICAO* [1997].

Table 2. Mean Daily Aircraft Movements Across the North Atlantic in Selected Periods

Route	Daily Movements in Both Directions in Period			
	November 1-7, 1994	July 1-7, 1995	July 1-7, 1997	November 1-7, 1997
Between Europe (without Iberia and Scandinavia) and North America	524	790	759	643
Total across the North Atlantic	693	893	1065	894

Most of the air traffic in the oceanic region is organized along the so-called Organized Track System (OTS) extending from 310 to 390 hft altitude and over a range of 5° to 6° latitude with 2000 feet (1000 feet since 1997) vertical and one degree latitude separation between individual flight tracks. For a given day, the corridor position is fixed about a day in advance and extends over about 6° in north-south direction. Individual aircraft fly with typically 20 min (15 min since 1997) time separation along the discrete tracks. A typical example is shown in Figure 3. This clearly defined structure enables focused measurements to be undertaken and provided sensitive tests of numerical models.

Plate 1 depicts the distribution of air traffic NO_x over the North Atlantic in the upper troposphere as calculated with the ECHAM3/CHEM model for the September-October period using the DLR-2 emission data base with a total of 0.56 Tg(N) yr^{-1} from aircraft NO_x emissions [*Köhler et al.*, 1997]. According to this climatological study the highest concentrations of aircraft NO_x are expected over the eastern North Atlantic and mid-Europe. Here the contribution of air traffic NO_x to the total NO_x abundance is on average about 40% for autumn conditions. Other models [e.g., *Kraus et al.*, 1996], with different emission estimates, predict slightly smaller values (30%).

2.2. The Experimental Carriers and Instrumentation

Measurements were performed using the research aircraft Falcon of DLR (Figure 4) and a B-747 combi airliner of type 357 of Swissair (Figure 5), see Table 3. Both aircraft cover the full altitude range of subsonic airliners and the expected altitude range of the tropopause in the NAFC [*Hoinka*, 1998]. The smaller Falcon jet covers the regional ranges. The larger DC-8 of NASA, see Figure 4, covered larger scales at slightly lower altitudes within the joint SONEX/POLINAT 2 experiment.

The Falcon and the B-747 aircraft were equipped with a large set of instruments. During the course of the projects, many of the instruments were new or had been improved relative to earlier versions. The Falcon was equipped with instruments measuring water vapor (H_2O) [*Ovarlez and van Velthoven*, 1997], ozone (O_3), carbon dioxide (CO_2), nitrogen oxides (NO, NO_x, and NO_y) [*Schlager et al.*, 1997a, b; *Ziereis et al.*, 1998a], nitrous acid (HNO_2), nitric acid (HNO_3), sulfur dioxide (SO_2), sulfuric acid (H_2SO_4), acetone ($(CH_3)_2CO$) [*Arnold et al.*, 1999; *Wohlfrom et al.*, 1999], carbon monoxide (CO), nonmethane hydrocarbons (NMHC, by grab samples), and photolysis rate of NO_2 [*Gerbig et al.*, 1996; *Slemr et al.*, 1998], total and nonvolatile (at 300°C) condensation nuclei (CN, that is, particles larger 5 nm in diameter), size spectrum

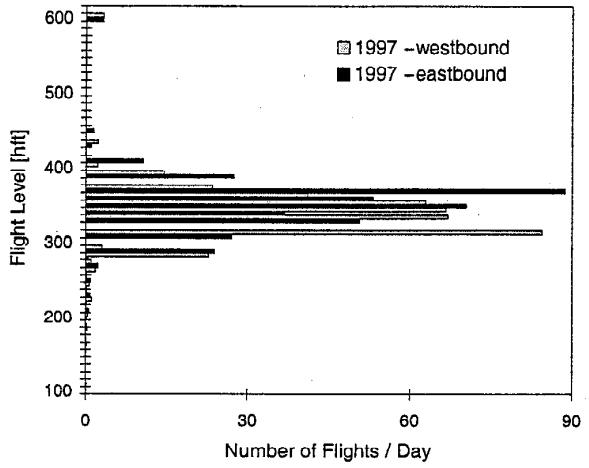

Figure 2. Vertical distribution of the number of aircraft per day passing the Shannon Air Traffic Control Area (45°-61°N, between 8.5° and 15°W) versus flight level (in hectofeet; 1 hft = 30.48 m) separately for eastbound and westbound flights during September 15 to 28 and October 10 to November 10, 1997 (data provided by Shannon Air Traffic Control Center and plotted by J. Freund).

and hydration properties of particles [*Hagen et al.*, 1996; *Paladino et al.*, 1998], meteorological parameters (pressure, temperature, humidity, wind components) and aircraft parameters (position, altitude, speed) [*Schumann et al.*, 1995]. The B-747 was equipped in the back cargo bay with a container including instruments to measure NO, NO_x, and O_3 [*Dias-Lalcaca et al.*, 1998]. Details on the instrumentation used on board the Falcon and B-747 are given in Table 4. The set of measurements helps to distinguish between species which were emitted by aircraft, transported upwards from the planetary boundary layer (PBL) or coming from the stratosphere [*Arnold et al.*, 1997a, *Schlager et al.*, 1997b].

2.3. Mission Strategy and Partner Missions

The rectangle in Plate 1 indicates the main Falcon operation area during POLINAT 1 and 2. The base of operations for the Falcon flights was Shannon International Airport (52°N; 10°W) in Ireland. The selected campaign site enables good latitudinal coverage of the flight corridor within the operation range of the Falcon and also allows difficult maneuvers in regions of high corridor traffic under radar control with assistance of Shannon Air Traffic Control. In addition, the B-747 sampled along the NAFC to search for longitudinal gradients in the abundance of air traffic related species.

The overall strategy of the POLINAT 1 experiment was to perform focused measurements in the NAFC during the main eastbound and westbound traffic flow, and to perform near-field plume measurements behind individual source aircraft. The strategy of POLINAT 2 experiment was to sample inside and outside of areas with expected high impact of aircraft emissions. This included measurements in the region with the highest air traffic density over the North Atlantic, vertical soundings through the flight corridor, and long-range flights from the center of the corridor to regions not or only weakly impacted by air traffic. The general flight pattern used during the Falcon missions included the following: perpendicular traverses of the corridor air traffic tracks; vertical and horizontal traverses of the (inclined) tropopause and measurements in the upper troposphere and lower stratosphere; vertical soundings including the range above and below the main flight corridor; southbound survey flights from Shannon to regions outside of the corridor (Azores and Tenerife); northbound survey flights from Shannon to the northern border of the flight corridor; traverses of regions with stagnant anticyclonic conditions; measurements within aircraft exhaust plumes (including the SONEX DC-8 and MOZAIC A340); formation flights with other research aircraft for instrument intercomparison; and coordinated measurements involving a large set of instruments and methods.

The SONEX campaign with objectives similar to those of POLINAT 2 was a key partner mission of the present investigations. The deployment of the Falcon and NASA DC-8, data exchange, and issues of data analysis and publication were coordinated as far as practicable. Selected missions of the Falcon were performed together with ACSOE and NARE flights, including intercomparison measurements with the MRF C-130 used for ACSOE, and an attempt of a Lagrangian experiment with the NOAA P3 deployed for NARE. Finally, a formation flight for instrument intercomparison was conducted of the Falcon and one instrumented Airbus 340 of MOZAIC.

2.4. Tools for Flight Planning

A large number of forecast products was transmitted to the field for flight planning. Meteorological products were available through KNMI [*Fuelberg et al.*, this issue; *van Velthoven*, 1999] including the following: isobaric maps (potential vorticity, wind, geopotential, humidity, temperature, etc.); forecasts of low, middle, and high cloud cover; forward/backward trajectories using ECMWF forecast winds; vertical cross sections of meteorological parameters along potential flight paths; and pressure map of dynamical tropopause for the North Atlantic region.

For the first time also chemical forecasts were available through UB/NILU including horizontal and vertical maps for a suite of air traffic related chemical species via an interactive webpage [F. Flatøy et al., unpublished manuscript, 1999]. Information on the location (e.g., Figure 3) and expected load of the OTS was available through Shannon Air Traffic Control. Preliminary NO_x and O_3 concentrations from past B-747

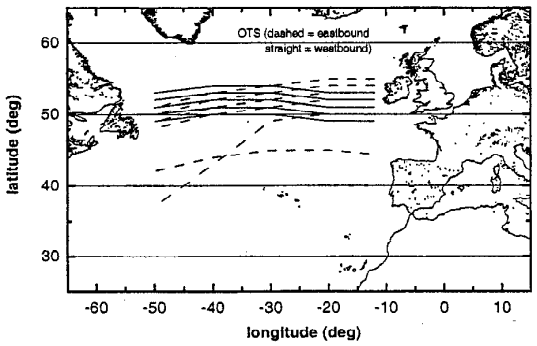

Figure 3. Westbound and eastbound oceanic organized track system (OTS) as of September 21, 1997.

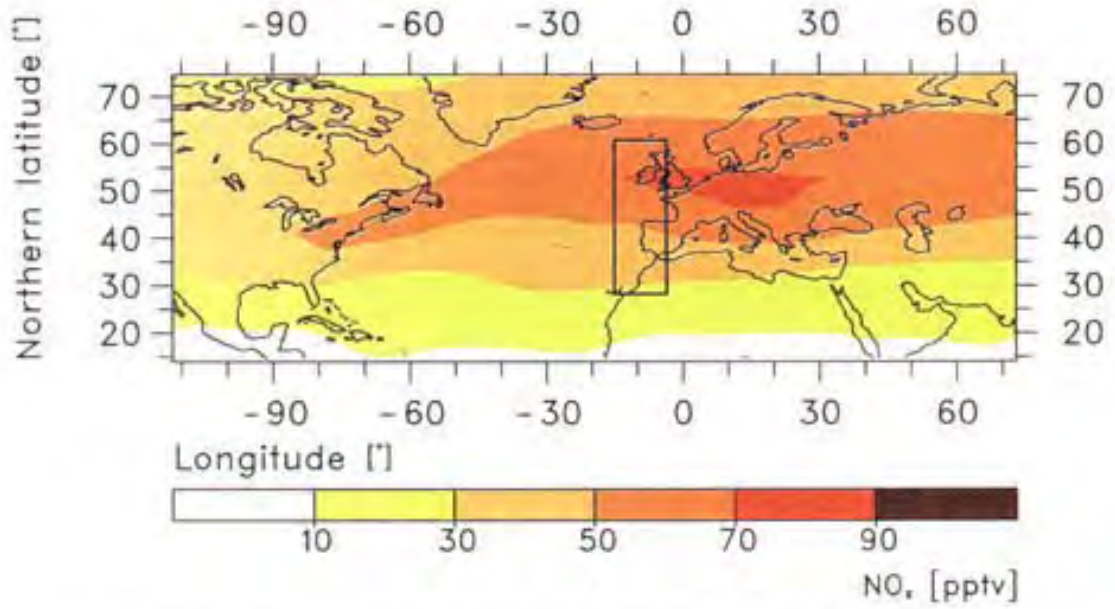

Plate 1. Mean distribution of air traffic induced NO_x at 200 hPa over the North Atlantic for September/October conditions from ECHAM3/CHEM studies [*Köhler et al.*, 1999]. The box indicates the main POLINAT 2 investigation area.

Figure 4. POLINAT 2/SONEX experimental team in front of the research aircraft DLR-Falcon and NASA-DC-8 on the airfield of Shannon, Ireland, during the experimental campaign in October 1997 (photo by M. Malycha. DLR).

Figure 5. The Swissair B-747 equipped with a container for measurements in the rear cargo compartment (photo provided by Swissair).

flights were made available via internet a few hours after landing of the B-747 in Zurich.

In addition, forecast products of SONEX could be used in October 1997, including 5-day history maps of air parcel encounters with the NAFC and regions with convective/lightning activity, respectively. These POLINAT and SONEX forecast products were used to characterize air masses prior to a mission with respect to an impact of air traffic, convection/lightning, boundary layer emissions, and stratospheric air.

2.5. Summary of the Experimental Missions

During the POLINAT 1 project, the Falcon covered the cross section of the flight corridor and sampled exhaust plumes at ages between minutes and several hours. Measurements have been made about 200 km west of Ireland, mainly along north-south flight legs of 300 km length at altitudes between 9 and 12 km, crossing the corridor. In the two series of experiments, eight measurement flights were performed under early winter conditions in November 1994 and nine under summer conditions in June/July 1995. The measurements covered the main traffic hours of westbound (around 12 to 15 UTC) and eastbound (6 to 9 UTC) flights. Shortly before and during some of the track crossing flights more than 100 airliners passed the measurement area.

POLINAT 2 covered the whole NAFC and its environment including measurements with the instrumented Swissair B-747 aircraft. The B-747 was operating out of Zürich, Switzerland. Figure 6 shows the flight tracks of the Falcon and the B-747 during POLINAT 2 together with those of the DC-8 during SONEX. POLINAT 2 covered early and late autumn conditions with 14 Falcon flights in two experimental phases (September 19 to 28 and October 14 to 23). In addition, the B-747 measured the distribution of nitrogen oxides and ozone during 98 traverses of the North Atlantic in the period from August 13 to November 23, 1997, thus providing comprehensive flight corridor concentration profiles during the whole POLINAT 2/SONEX campaigns. The POLINAT 2 campaign period took place during a time of year with weakened impact of deep convection and lightning on the NO_x distribution over the eastern North Atlantic but still with substantial photochemical activity. The tropopause altitude varied longitudinally with local maxima (ridges) at 5°E and 50°W, and clear downward trend from south to north. At 35°N, only about 10% of the B-747 measurements were taken above the tropopause, while at 55°N half of them were taken above the tropopause.

Table 5 summarizes the dates of the Falcon flights and the general objectives of the missions. The rationales and general flight pattern of the Falcon missions are detailed by *Schlager et al.* [1997a, b, 1999].

The data measured during POLINAT 1 and 2 by the Falcon and the B-747 are archived in one common data bank in a format as used also within SONEX and other NASA and European projects. The data can be made available by ftp or on a compact disk. The POLINAT 2 data are also included in the SONEX data bank, see http://www.pa.op.dlr.de/polinat/ or http://telsci.arc.nasa.gov/~sonex/.

3. Modeling

Several existing global, regional, and plume scale models were further refined and applied for analysis of the measured results. The models are listed in Table 6, together with a short identification of their content, scales, usage within POLINAT, and references. The models have been applied to investigate the impact of aircraft emissions on the state of the atmosphere at all scales from the plume to the global scales (e.g., Plate 1). The results of all models have been compared with experimental results. The models are used to study the conversion of emissions and particle formation in the aircraft plume, including plumes from several aircraft flying the same route ("multiple plumes"), and the impact of aircraft emissions on air composition at various scales up to the globe relative to other sources of the modeled trace gases.

The chemical transport model NILU-CTM has been used for prediction of air chemistry during the experimental periods. For this purpose, the model used annual mean aircraft emissions [*Gardner*, 1998]. Plate 2 shows, for example, the prognoses for October 20, 1997. In this example, a large fraction of the NO_x, in particular over England and central Europe and over the eastern United States of America, result from aircraft emissions in this model for this day, while other emissions have been transported out of the NAFC region over a large distance. Such data provided clear indication where to measure to find aircraft traces [see *Schlager et al.*, 1999].

4. Major Results

With respect to the questions stated in the Introduction, the following answers have been derived from the studies performed:

4.1. What is the Mean Abundance of Aircraft-Emitted Species and Other Related Species Vertically and Horizontally Across and Along the Corridor?

Figure 7 shows the data obtained from all Falcon flights excluding near-field plume observations during POLINAT as a

Table 3. Aircraft, Their Maximum Ceiling, Range, and Speed During POLINAT 2 and SONEX

Aircraft	Ceiling Altitude, km	Range, km	Speed, m s^{-1}
Falcon	13.1	3500	180-225
B-747	12	7100	250
DC-8	11.9	6800	200-250

Table 4. POLINAT 2 Instruments and Measurements With Typical Accuracies

Species	Technique	Group	Accuracy	Primary (XX) and Secondary (X) Tracer for		
				Aircraft Emissions	PBL Air	Strato-spheric Air
		Falcon				
NO/NO_2	CL/UV photolysis	DLR	±15/25%	XX	X	
NO_y	CL/Au converter	DLR	±20%	XX		XX
HNO_2/HNO_3	CIMS	MPI-K	±30%	X		XX
O_3	UV absorption	DLR	±5%			XX
CO_2	IR absorption	DLR	±0.5ppm	XX	X	
CO	VUV fluorescence	IFU	±15%		XX	X
H_2O	frost point / cryo-genic	LMD	±5%	X		XX
$(CH_3)_2CO$	CIMS	MPI-K	±30%		X	
HC (C1-C8)	grab sample/GC	IFU	±8-20%		XX	
SO_2	CIMS	MPI-K	±30%	X	XX	
H_2SO_4	CIMS	MPI-K	±30%	X		XX
$j(NO_2)$	actinometry	IFU	±15%			
Aerosol size	EAC	UMR	±20%	X		
CN_{tot}/CN_{nv}	counter/heated inlet	UMR	±15%	XX	X	X
		B-747				
NO/NO_2	CL/UV photolysis	ETH	±15/30%	XX	X	
O_3	UV absorption	ETH	±5%			XX

function of altitude. Figure 8 depicts all Falcon NO, NO_x and NO_y data obtained during the 1997 flights when the instruments measured NO_x and NO_y simultaneously with NO. The figures depict the range of data collected and the variability within the results obtained. The measurements cover the upper troposphere and the lowermost stratosphere between 28°N-62°N and 10°E-25°W, see Figure 6, with the bulk of data from 49°-57°N, 5°-15°W. The Falcon climbed up to 13.1 km in 1997 and up to 12.5 km in 1994/1995. It often flew above the local tropopause (deduced from the vertical temperature lapse rate) by a few kilometers, in particular in the November 1994 period where the tropopause occasionally reached below 6 km, and performed measurements in the lowest layers of the stratosphere characterized by values of the potential vorticity (explained, e.g., by *Hoinka et al.* [1993]) of up to 10 PVU (1 PVU = 1 potential vorticity unit = 10^{-6} K m^2 kg^{-1} s^{-1}), potential temperature T_{pot} ($T_{pot} = T\,(p_0/p)^{\kappa}$, p_0 = 1013.25 hPa, κ= 0.286) up to 365 K, O_3 mixing ratios up to 400 ppbv (1 ppbv = 1 parts per billion by volume = 1 nmol mol^{-1}), and water vapor mixing ratio down to 6 ppmv (1 ppmv = 1 parts per million by volume = 1 μmol mol^{-1}). In stratospheric air masses (e.g., defined by more than 130 ppbv O_3 mixing ratio or more than 3 PVU potential vorticity), H_2O, CO, acetone, and particle concentrations decrease with altitude. CO_2 mixing ratios (355 to 366 ppm) are higher above than below the tropopause due to a phase shift in the seasonal cycle of the CO_2 abundance in the lowermost stratosphere and the upper troposphere. Within the troposphere (defined, e.g., by less than 1.5 PVU potential vorticity or less than 80 ppbv O_3 mixing ratio), H_2O, CO, total, and nonvolatile CN particle concentration values are significantly higher than in the lower stratosphere, as expected. The increase in CO concentration with altitude within the midtroposphere is atypical [*Hauglustaine et al.*, 1998] and may reflect different origins of the air masses at different altitudes and some contribution from oxidation of methane.

The measured NO_x, HNO_3, SO_2, and $(CH_3)_2CO$ abundances (outside young aircraft plumes) show large variability in the upper troposphere. The mixing ratios of these species vary

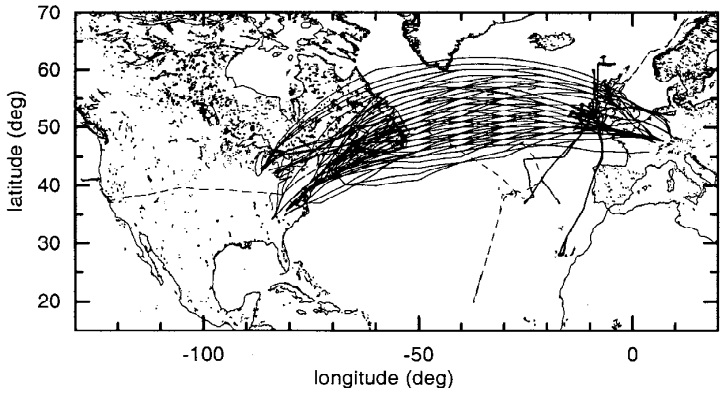

Figure 6. Flight tracks of the Falcon (thick full curves) west of Ireland and the B-747 (thin full curves) between Europe and North America during POLINAT 2 and the DC-8 (dashed) during SONEX (provided by P. Schulte).

Table 5. Summary of Falcon Flights During POLINAT

Phase	Flight Outline
POLINAT 1, Early Winter, November 1994	
N1, Nov. 2	instrument/flight procedure test, air traffic plumes
N2, Nov. 3	corridor measurements, air traffic plumes
N3, Nov. 5	tropopause fold crossing
N4, Nov. 6	corridor measurements, air traffic plumes
N5, Nov. 8	detection of boundary layer air
N6, Nov. 10	corridor measurements, air traffic plumes
N7, Nov. 11	near-field plume measurements
N8, Nov. 13	near-field plume measurements
POLINAT 1, Summer, June/July 1995	
P1, June 21	corridor measurements, air traffic plumes
P2, June 24	accumulation in stagnant anticyclone
P3a, June 26	large-scale trace gas distribution and
P3b, June 26	accumulation in stagnant anticyclone
P4, June 28	accumulation in stagnant anticyclone
P5, June 30	near-field plume measurements
P6, July 1	thunderstorm signatures
P7, July 3	near-field plume measurements
P8, July 5	near-field plume measurements at night
POLINAT 2, Early Autumn, September 1997	
F1, Sept. 19	northbound corridor survey
F2, F3, Sept. 21	southbound survey to Azores, intercomparison with C130, intersection of boundary layer air from United States of America
F4, Sept. 24	persistent contrails, MOZAIC intercomparison + plume sniff
F5, Sept. 26	stagnant anticyclone, Lagrangian experiment with NOAA P3
F6, F7, Sept. 28	Falcon/B-747 intercomparison, northbound corridor survey, Lagrangian experiment with NOAA P3
POLINAT 2, Late Autumn, October 1997	
F8, F9, Oct. 14	southbound survey to Tenerife
F10, Oct. 18	corridor track crossings and intercomparison with SONEX
F11, F12, Oct. 20	southbound survey with SONEX
F13, Oct. 23	corridor track crossings with SONEX, DC-8 intercomparison including DC-8 exhaust plume sniff

over more than 2 orders of magnitude. Measured NO values often exceed 0.7 ppbv, and H_2O vapor concentrations range between 6 and more than 2000 ppmv [*Ovarlez and van Velthoven*, 1997]. The H_2O mixing ratio decreases with altitude and varies above the tropopause (at PV > 3.5 PVU) between 6 and 50 ppmv in winter and between 15 and 50 ppmv in summer, consistent with transport from the tropopause to the stratosphere at middle and high latitudes [*Ovarlez et al.*, 1999]. The concentration of HNO_3 varies between 0.01 and about 2 ppbv [*Schneider et al.*, 1998], SO_2 between 0.01 and 1.5 ppbv, and $(CH_3)_2CO$ between 0.1 and 2 ppbv [*Arnold et al.*, 1997b]. The acetone abundance found is often larger than measured before over the Pacific where mean values of the order of 600 pptv were reported for the middle and upper troposphere at northern midlatitudes [*Singh et al.*, 1998]. Some of the data show seasonal differences with mean values varying by a factor of the order of 2. The median NO mixing ratio values near the tropopause were largest in the June/July period and smallest in November. Acetone was largest in the summer 1995 and autumn 1997 cases, SO_2 and HNO_3 were smallest in the 1997 period. Measurements of HNO_2 (only within aircraft plumes) [*Arnold et al.*, 1992; *Tremmel et al.*, 1998], H_2SO_4, CH_3CN, and HCN have been obtained. The observed number density of gaseous H_2SO_4 ranges from about 1×10^5 to 3×10^6 cm^{-3} with a mean value of roughly 5×10^5 cm^{-3} [*Arnold et al.*, 1999].

The vertical NO, NO_x, and NO_y profiles, see Figures 7 and 8, show local maxima near 10.5 to 11.5 km altitude, occasionally exceeding 2.5 ppbv. The profiles are different from the C-shaped profiles observed elsewhere [*Drummond et al.*, 1988; *Hauglustaine et al.*, 1998]. At all latitudes, no significant vertical gradient of NO is found near the tropopause. The mean values of NO concentrations are rather large and vary between 100 and 140 pptv in summer and 30 and 100 pptv in late autumn [*Ziereis et al.*, 1999a, b, this issue]. The local maxima occur at the altitudes of major air traffic levels, regardless of whether the air mass is of tropospheric or stratospheric origin. During POLINAT 2, the mean and the median values (in ppbv) in the altitude range from 10.5 to 11.5 km are 0.14, 0.22, 0.59 and 0.09, 0.14, 0.34 for NO, NO_x, NO_y, respectively. Hence more than 64% of the observed NO_x is made up of NO, and more than 40% of the NO_y is NO_x in this altitude range. The large NO/NO_x ratio reflects the strong photolysis rate, low temperature and still rather low O_3 mixing ratio at these altitudes [*Schlager et al.*, 1997b; *Ziereis et al.*, 1999a]. The large NO_x/NO_y ratio indicates a large fraction of fresh NO_x emissions. Some of the NO_x peaks may be due to the fact that most of the measurements were made within the center of the NAFC where there is a higher probability of encountering air masses polluted by aircraft.

A marked latitudinal gradient in NO, NO_x, and NO_y was observed near 0°W. Mean NO volume mixing ratios in the upper troposphere increased from a few tens of pptv near 30°N to about 200 pptv near 60°N. A similar gradient was found for NO_y but not for CO. In the northern part of the POLINAT 2 measuring area the NO and NO_x mixing ratios increase with altitude and are maximum near the tropopause while in the southern part only a weak altitude gradient was observed. On average over all latitudes, about 20 to 30% of the observed NO_y is made up of NO_x [*Ziereis et al.*, 1999a, this issue].

The B-747 based measurements provided a representative picture of O_3 and NO_x concentrations in the NAFC. At cruise altitudes (190-300 hPa, 12.1-9.2 km) the NO_x concentrations obtained between September and November in the years 1995 and 1997 were very similar and ranged from 100 to 150 pptv over the North Atlantic (40°-60°N and 10°-40°W) and between 190 and 280 pptv above the continental United States of America (30°-60°N and 60°-90°W) [*Jeker et al.*, this issue]. The POLINAT 2 project results therefore confirm and extend those obtained during the Swiss project NOXAR in 1995 and 1996 [*Brunner*, 1998; *Brunner et al.*, 1998]. The NO_x abundance measured onboard the B-747 shows mixing ratio values versus flight time with many short-period (3 to 30 s) peaks often exceeding 3 ppbv, obviously from aircraft emissions, and wider peaks exceeding 0.5 ppbv (often above 1 ppbv) over more than 500 km distance, reflecting upward convection of polluted boundary layer air masses or lightning contributions. Plate 3 depicts the daytime NO_x concentration field as measured during NOXAR in July 1995, temporally overlapping the POLINAT 1 measurement period, in comparison to model analyses performed within POLINAT. The measured data are discussed by *Brunner et al.* [1998]. We note a strong east-west gradient with NO_x values up to 600 pptv east of the North American continent, a reduction to values of about 200 pptv over the mid North Atlantic and a slight increase by about 50 pptv over the British Islands. The data give a weak indication

Table 6. Models, Their Objectives, Scales, and Operating Groups and References, as Used Within the POLINAT Projects

Model Name	Model Domain and Objectives	Scales	Group	References
		Global		
ECHAM3/ NOX and CHEM	global circulation model with simplified (NOX) or more complete chemistry (CHEM): (a) analysis of impact of convective transport and washout of nitric acid, (b) analysis of NO_x statistics, (c) chemical effects on ozone	3-D, global, T21 (5.6° x 5.6°), 19 layers up to 10 hPa	DLR	*Köhler et al.* [1997] and *Steil et al.* [1998]
TM3-KNMI	Chemical Transport Model (CTM): (a) analysis of aircraft impact for anticyclone conditions, (b) impact of emissions on ozone chemistry	3-D, global, 3.75° x 5°, 19 levels up to 10hPa	KNMI	*Wauben et al.* [1997a]
STOCHEM	chemical Lagrangian transport model: impact of emissions on ozone chemistry	3-D, global, 10° x 10°, 9 levels up to 16 km	Met. Office	*Stevenson et al.* [1997]
PATCHM	global semi-Lagrangian transport model: Impact of emissions on ozone chemistry	3-D, global, 5° x 5°, 10 levels up to 16 km	AEA	Hayman *et al.* [1999]
		Regional		
NILU-CTM	analysis and prediction of chemical fields of the North Atlantic using ECMWF prediction and analysis fields for experiment planning and analysis	North Atlantic, 10 or 18 layers up to 100 hPa, nested models, 50 or 150 km grid	Univ. of Bergen and NILU	*Flatøy and Hov* [1996, 1997]
MACHO	CTM for tropospheric chemistry: analysis of parameters controlling regional impact of NO_x on ozone	3-D, 50 km grid, 20 layers up to 100 hPa. Lateral boundary concentrations from the global Oslo CTM2 at T21 resolution	Univ. of Oslo	*Jonson et al.* [1999a]
		Plume Scale		
NILU plume chemistry model	expanding plume model with several radial rings, with gas and aerosol chemistry: impact of small-scale mixing and chemistry in multiple plumes on ozone chemistry	1-D, 8 radial rings, following trajectories	NILU	*Kraabøl et al.* [1999]
AEA/UCL aerosol model	flow field simulation: temperature in jet exhaust for nucleation physics	2-D	AEA	*Ford et al.* [1999]
AEA plume chemistry model	plume chemistry with aerosols, and hydrocarbons: impact of emissions, mixing and background on plume chemistry, effective emissions in aged plumes, impact of hydrocarbon and chlorine chemistry	2-D, puff along trajectory	AEA and Univ. College London	*Hayman and Markiewicz* [1997]
Gaussian	Gaussian plumes model: analysis for plume dispersion for single and multiple plumes, comparison with plume measurements	3-D (analytically), within a vertical corridor cross section of 1000 km x 5 km	DLR	*Schumann and Konopka* [1994]
LESTUF	large-eddy simulation of turbulent flows: effective vertical and horizontal diffusivities and plume dispersion in stable and sheared environments	3-D, 10 km x 3 km x 3 km, 400 x 100 x 30 cells	DLR	*Gerz et al.* [1998]

for a ridge of enhanced NO_x (with more than 200 pptv) within parts of the NAFC passing Iceland and Newfoundland compared to values between 150 and 200 pptv outside this corridor. Similar data for September-November 1995 show lower NO_x values (maximum 300 pptv over the southeast United States of America) with a mean of 150 pptv over Ireland, and slight indication for a ridge of NO_x values between 120 and 150 pptv over most of the NAFC east of 45°W with smaller values (about 100 pptv) north and south of it. The comparison with the model data will be discussed below.

Particle measurements include the number concentration CN of small particles larger than 5 nm, the size distribution of aerosol (DMA, differential mobility analyzers), the volatility (with respect to thermal evaporation at 300°C), and the soluble mass fraction (deliquescence with tandem DMA). The aerosol size spectra often show a Junge-type distribution with monotonic exponential decrease of the number density in the diameter range from 4 to 300 nm. The size spectrum of the water-soluble aerosol, both inside and outside of the corridor, generally displayed a unimodal structure with a peak below 25% soluble mass fraction. By comparing CN concentrations from heated and unheated inlets, the ratio of volatile to involatile aerosols was measured. Typical values are 3:1 in the background and up to 50:1 in moderately aged exhaust plumes [*Hagen et al.*, 1996; *Paladino et al.*, this issue].

4.2. What are the Effective Emissions, Dispersion, Chemical Conversion, and Particle Formation in Single and Multiple Plumes From One or Several Aircraft?

During POLINAT 1, effective emission indices (EI) of NO_x, HNO_2, HNO_3, SO_2, total and volatile CN have been measured for a set of 11 wide-body aircraft, see Table 7, for ambient atmospheric conditions as listed in Table 8. The emission index values are derived from the ratio of the concentration above background of the emitted species relative to that of CO_2 with known emission index (about 3.15) [*Schulte and Schlager*, 1996]. Figure 9 collects all values from POLINAT and other measurements available for direct comparison of measured and computed EI(NO_x). The values of EI(NO_x) vary between 12 and 30 g(NO_2) per kg fuel burnt for long range aircraft with different engine types and ages [*Schulte et al.*, 1997; *IPCC*, 1999, p. 252]. These EI values are larger than those of medium range aircraft (8-13 g kg^{-1}). The measured values appear to be 10 to 20% higher than the computed values. Similar differences were found recently in measurements of EI(NO) and EI(NO_y) by *Campos et al.* [1998]. The observations include five B-747/JT9D cases, and are consistent with the large EI-values expected for this combination [*Gardner et al.*, 1997], but many of these relatively old aircraft/engine

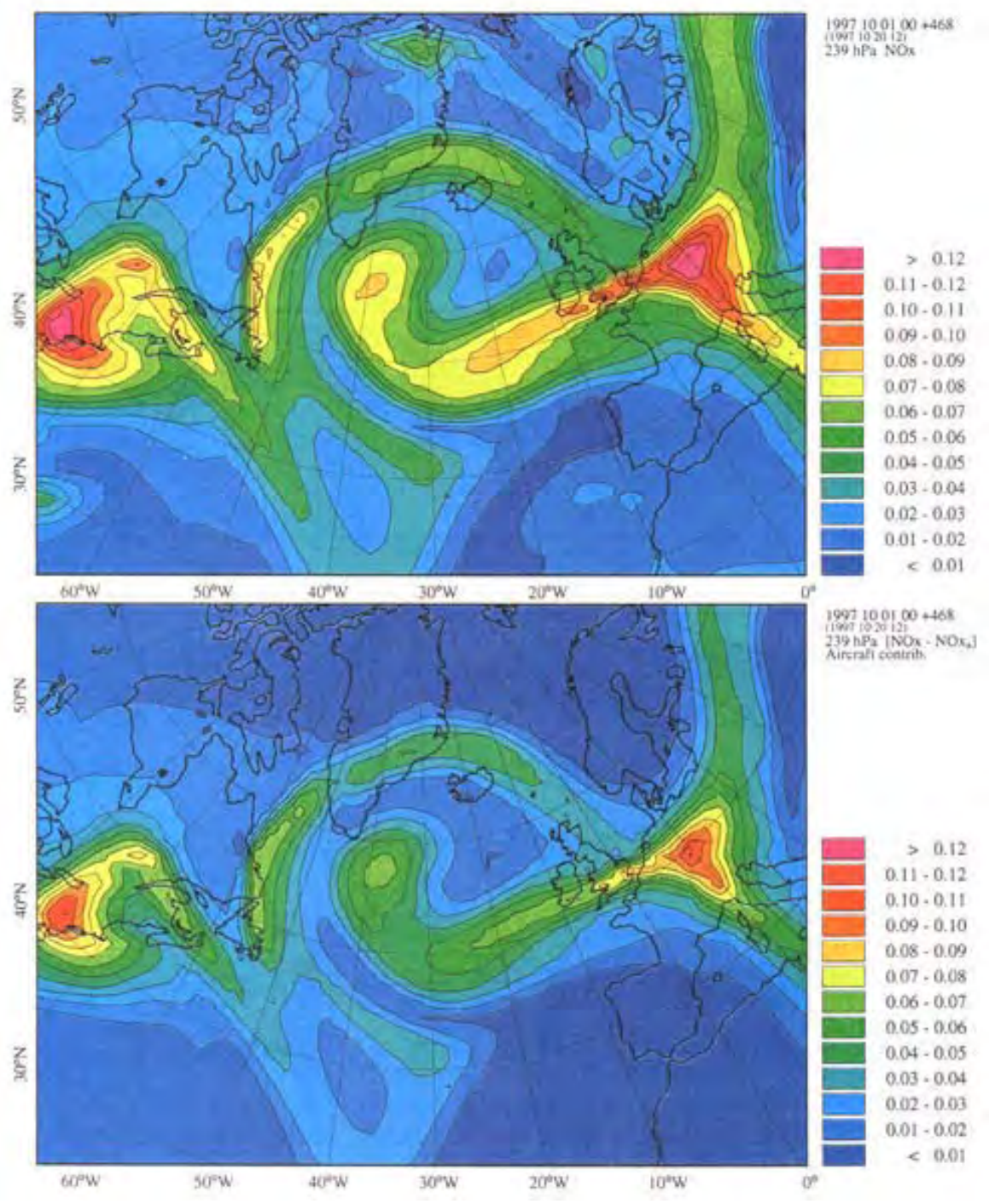

Plate 2. Example of the 48-hour chemistry forecast provided by UB/NILU via internet for 1200 UT October 20, 1997. Results are shown at 239 hPa (10.65 km) for NO_x (top) from all sources and (bottom) from aircraft induced NO_x alone. (Provided by F. Flatøy).

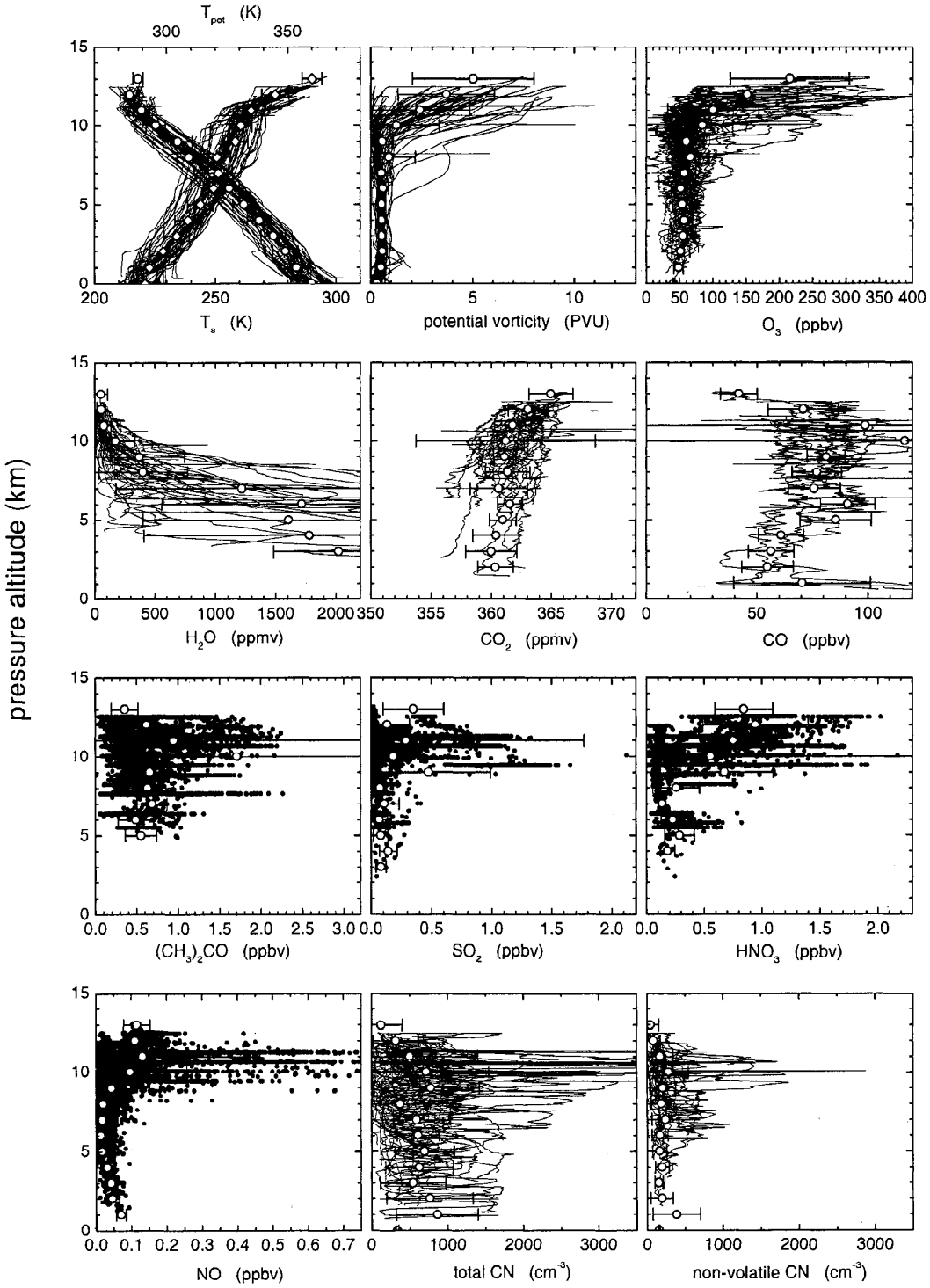

Figure 7. Measured values of temperature, potential temperature, potential vorticity, mixing ratios of O_3, H_2O, CO_2, CO, $(CH_3)_2CO$, SO_2, HNO_3, NO, concentrations of total condensation nuclei (CN), and nonvolatile CN versus pressure altitude from all POLINAT flights in the NAFC domain in 1994, 1995, and 1997. The individual data points or profile lines represent 10 s mean values. The open circle with error bars represent mean values over 1 km altitude intervals and the standard deviation (provided by P. Schulte).

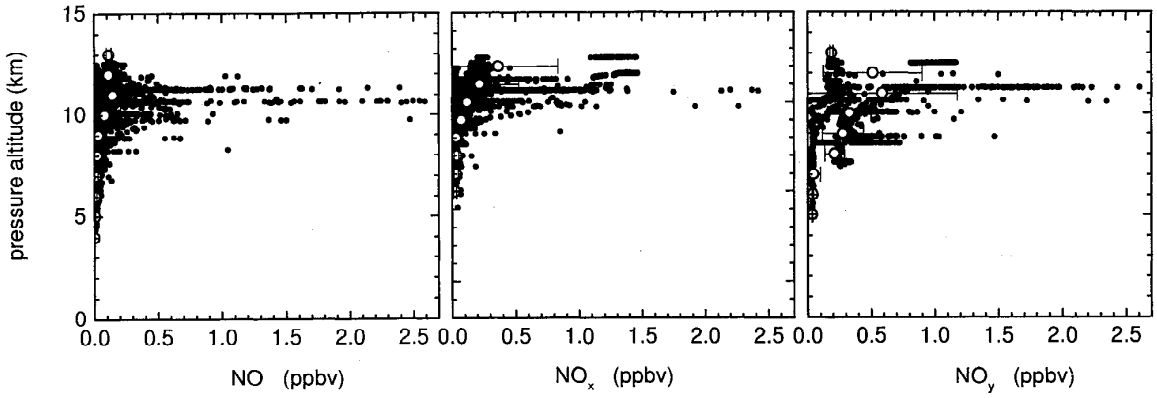

Figure 8. Measured values of NO, NO_x, and NO_y mixing ratios (dots, 10 s mean values) versus pressure altitude from POLINAT 2 flights in the NAFC domain in 1997. The open circle with error bars denotes the mean values over 1 km altitude intervals and the standard deviation (provided by P. Schulte).

combinations are presently being replaced with more modern versions.

For the DC-8 case, the Falcon stayed long enough in the young exhaust plume (plume age order of 1 s) to get reliable plume increases of H_2O and the deduced EI value of 1.28 was close to the value expected (1.23 to 1.26, depending on the hydrogen content of the fuel). (The plume NO concentration exceeded the instrument range preventing measurements of EI(NO_x) in this case.)

The measured EI(SO_2) range between 0.2 and 0.8 g kg^{-1} for different aircraft, which reflects typical variations in fuel sulfur contents [*Brasseur et al.*, 1998]. Obviously, only part of the SO_2 gets converted into aerosol. The effective EI for HNO_3 and HNO_2 at plume ages of the order of 100 s vary between 0.06 and 0.4 g kg^{-1}, see Table 7 and *Tremmel et al.* [1998]. Inferred EI(OH) are about 0.3 to 1 g kg^{-1}.

Aircraft cause CN particle EI values of the order of 10^{16} per kg burnt fuel mass, but the numbers vary strongly from engine to engine, depend on the lower cut-off size of the CN counters, and possibly other parameters [*Paladino et al.*, 1998; *Schröder et al.*, 1998]. Particle measurements in the young exhaust plume of the SONEX DC-8 revealed only 10^{13} nonvolatile particles per kg fuel [*Paladino et al.*, this issue]. About 90% of the measured particles are volatile, consistent with previous findings [*Kärcher et al.*, 1998]. As shown by direct measurements [*Curtius et al.*, 1998], the volatile plume particles contain H_2SO_4. The data suggest mean increases in CN concentrations in the NAFC of the order of 30 cm^{-3} (typical background concentrations are 100 to 500 cm^{-3}) [*Schlager et al.*, 1997b].

Less than 10% of the emitted NO_x, depending on the oxidizing properties of the ambient air, gets converted to HNO_3 within the first hours [*Klemm et al.*, 1998]. Direct HNO_2 and HNO_3 measurements during November in plumes at about 100 s age show conversion fractions of the order of 1% [*Tremmel et al.*, 1998]. In the winter and summer cases, plume model studies show that after 10 hours, about 4% and 10%, respectively, of the emitted NO_x is converted to reservoir species (mainly HNO_3). Slow dispersion and large concentration of nitrogen oxides in multiple plumes from contributions of several aircraft flying through essentially the same air mass reduces the chemical conversion of NO_x to HNO_3 and the photochemical ozone production rate compared to single plumes [*Kraabøl et al.*, 1999]. As a consequence, the emissions into multiple plumes have smaller impact on O_3 formation than from individual and quickly diluting plumes [*Meijer et al.*, 1997; *Petry et al.*, 1998].

A new aerosol model has been set-up which computes the formation of sulfuric acid, homogeneous binary nucleation, coagulation, interaction with soot aerosol, and mixing with ambient air [*Ford et al.*, 1999]. The model was coupled to a wake vortex flow model. Particle nucleation and ice particle formation are found to be surprisingly insensitive to the rate of aerosol nucleation used in models. This is because of the rapid rise in supersaturation due to cooling, followed by the depletion of the vapor phase by the nucleation of new particles. The nucleation burst self-terminates. Hence the number of aerosol particles formed depends on atmospheric conditions and plume mixing rates but not strongly on the fuel sulfur content and very little on the actual details of the nucleation process. In aircraft plumes, the rate of freezing nucleation is often so much faster than particle growth that the effect of different growth of liquid and frozen particles broadens the size distribution slightly but does not result in a bimodal size distribution [*Ford*, 1999a, b].

Computations with an expanding plume model with chemistry have shown that contrails forming at ice supersaturated ambient air conditions and cirrus particles provide enough surface for heterogeneous chemistry to reduce the O_3 increase, which is computed for pure gas chemistry, by activation of chlorine compounds [*Kraabøl et al.*, 1999]. In plumes too dry to form contrails, the impact of heterogeneous reactions was found to be negligible. A plume chemistry model including reactions with the emitted hydrocarbons revealed small impact of the emitted hydrocarbons on ozone chemistry in the plume [*Hayman and Markiewicz*, 1997].

4.3. At What Time Scales and Space Scales do the Pollutants Become Homogeneously Mixed?

The emissions from air traffic are clearly measurable in terms of the increases in the concentrations of NO_x, HNO_2, HNO_3, SO_2, H_2O, particles and CO_2 observed within individual aircraft exhaust plumes. The plume concentrations com-

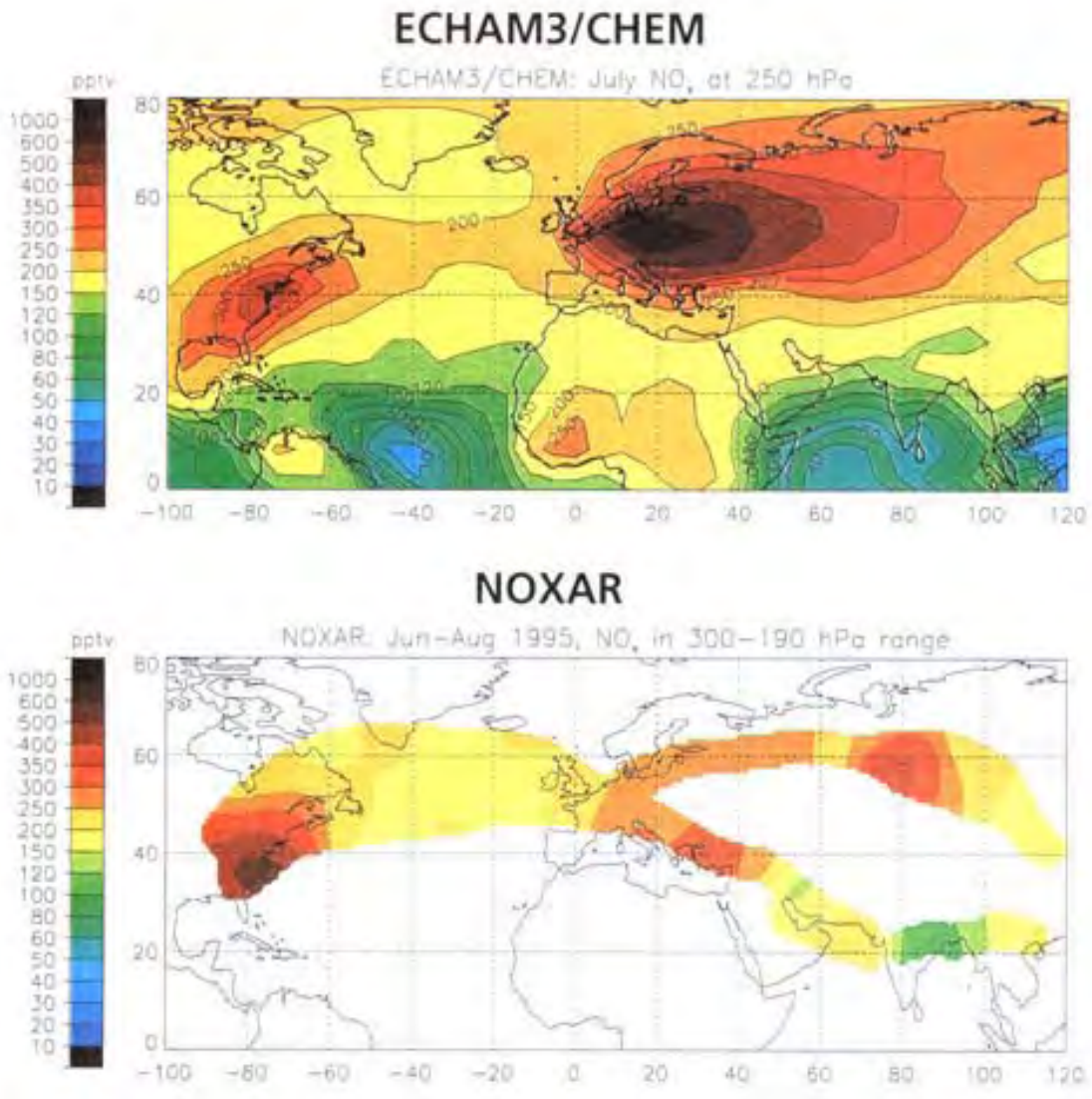

Plate 3. Daytime NO_x concentration distribution at cruising altitude in the range of the Swissair B-747 versus latitude and longitude [*Brunner*, 1998]. (top) ECHAM3/CHEM results at 250 hPa. (bottom) NOXAR results with all 2 min averaged samples taken at 190-300 hPa from June to August 1995. The color coding ranges from 0 (black, followed by blue) to more than 1000 pptv (dark red and black), plotted by D. Brunner with ECHAM3 data by V. Grewe and I. Köhler.

Table 7. Emission Indices for Long-Range Aircraft

Case	Type	Engine	EI NO_x, g kg^{-1}	EI HNO_2, g kg^{-1}	EI HNO_3, g kg^{-1}	NO/NO_x, $\gamma(\tau)$	NO/NO_x, $\gamma(0)$	EI OH, g kg^{-1}	EI SO_2, g kg^{-1}	EI total, 10^{15}/kg	EI nonvolatiles, 10^{15}/kg	EI volatiles 10^{15}/kg
1	B747-400	CF6-80C2B1F	12.3	-	-	0.06	0.03	-	-	-	-	
2	B747-100	JT9D-7A	(18.1/18.1)	0.81	0.80	(0.12	0.14/0.17	0.36/0.39	0.32	-	0.89	
3	B747-100	JT9D-7A	(26.1/26.8)	0.44	0.17	(0.12)	0.12/0.16	0.32/0.34	0.17	-	0.33	
4	B747-200B	CF6-50E2	14.9	-	-	(0.15)	(0.07)	-	-	-	0.54	
5	B747-200B	JT9D-7J	23.7	0.14	0.15	0.09	0.15	0.11	0.48	3.8	0.27	3.4, 3.6
6	DC10-30	CF6-50C	19.7	-	0.13	0.11	0.07	0.24	0.53	10.6	0.46	10.1
7	B747-200B	JT9D-7J	30.4	0.30	0.33	0.06	0.15	0.28	0.52	8.7	0.45	8.4, 8.1
8	B747-100	JT9D-7A	21.0	0.10	0.06	0.07	0.13	0.06	0.20	0.81	0.57	
9	B747-200B	CF6-50E2	17.0	-	-	0.23	0.15	-	-	0.9	0.53	0.4, 0.5
10	A340-300	CFM56-5C2	16.2	-	-	0.22	0.10	-	(0.96)	22.9	1.6	23.0, 19.6
11	A340		-	-	-	-	-	-	-	-	-	-
12	DC-8	CFM 56-2-C1		0.17	0.06	-	0.3	0.08	0.46 (1.38)	-	0.011	-

Emission indices (EI) of gases and particles. The EI(NO_x) data for cases 1 to 10 have been deduced by *Schulte et al.* [1997]. That paper gives more details on these cases. The OH indices for cases 2 and 3 and related data are taken from *Tremmel et al.* [1998], details on the emission indices for particles are explained by *Paladino et al.* [this issue] and *Konopka et al.* [1997]. Case 11 is described by *Helten et al.* [1999], and case 12 is described by *Arnold et al.* [1999]. Values of EI(NO_x) in brackets are computed from the measured NO emissions, a plume chemistry model, and an assumed initial NO/NO_x ratio at engine exit of 0.07. Double entries for EI(OH) and NO/NO_x refer to the conditions at engine exit and at combustor exit. For case 10 and 12, the SO_2-emission index is derived from the measured fuel-sulfur content (480 and 690 g kg^{-1}) assuming 100% conversion to SO_2.

pare well with models following the dispersion from individual aircraft. Often, the measured plumes result from a superposition of several aircraft exhaust plumes [*Schlager et al.*, 1997b]. The expected titration of O_3 by fresh NO emissions from aircraft in plumes at ages of minutes [*Brasseur et al.*, 1998] is often less than the scatter of background O_3 concentration and hence too small to be measurable.

Visual observations of contrails and measurements of various emissions concentration and turbulence within aircraft exhaust plumes give important insight into the motions and mixing during the vortex and dispersion phases of the plumes. A double vortex system forms behind aircraft and sinks downward. It carries exhaust typically 150 to 200 m below the flight level. Part of the emissions leave the vortex system and form a curtain of emissions between the flight level and the sinking vortex pair [*Gerz et al.*, 1998]. Maximum NO_x concentrations were measured within the centers of the vortex pair [*Schlager et al.*, 1997a; *Brasseur et al.*, 1998]. The vortex motion breaks up into turbulent motions before the vortex air rises back to the flight level. Hence most of the emissions get deposited below the flight level [*Gerz et al.*, 1998] and the measurements which were often performed at the flight levels of cruising airliners may underestimate the concentration increase caused by these aircraft.

The measurements and models confirmed expectations [*Schumann and Konopka*, 1994] in showing that air traffic emissions cause a very peaky distribution of the concentration fields in the flight corridor, in particular for NO_x and particles. It takes about 3 to 10 hours before individual plumes get diluted to background NO_x concentration values within the range of variance of the background values [*Schlager et al.*, 1997b]. At this time scale, plumes extend typically 200 m vertically and 15 km laterally. After decay of the aircraft induced vortex system, the plumes experience far less vertical than horizontal dispersion, depending mainly on stratification and vertical shear of the cross-plume wind field [*Schumann et al.*, 1995; *Dürbeck and Gerz*, 1995, 1996].

In spite of the complex mixing behavior, the dilution of exhaust plumes follows a simple dilution law within a standard deviation of the logarithmic values corresponding to a factor

Table 8. Atmospheric Conditions During Measurements Behind Long-Range Aircraft

Case	p, hPa	T, °C	RH, %	T_c, °C	Contrail seen
1	216.6	-57	32	-50.9	yes
2	266.9	-48	18	-49.5	no
3	300.9	-42	11	-48.6	no
4	238.4	-53	24	-50.4	yes
5	262.0	-46	17	-49.7	no
6	262.0	-45	18	-49.7	no
7	262.0	-45	21	-49.6	no
8	262.0	-45	19	-49.7	no
9	238.4	-51	27	-50.2	yes
10	238.4	-51	29	-50.1	yes
11	238.4	-54	65	-48.2	yes
12	261	-49	57	-47.8	yes

Ambient pressure (p), temperature (T), relative humidity of liquid saturation (RH), contrail threshold temperature (T_c), and report on whether a contrail was seen or not. Cases as in Table 7. The computations of T_c are performed using the revised Schmidt/Appleman criterion with propulsion efficiency $\eta = 0.33$, water vapor emission index $EI_{H2O} = 1.25$, and fuel combustion heat $Q = 43$ MJ kg^{-1} [*Schumann*, 1996].

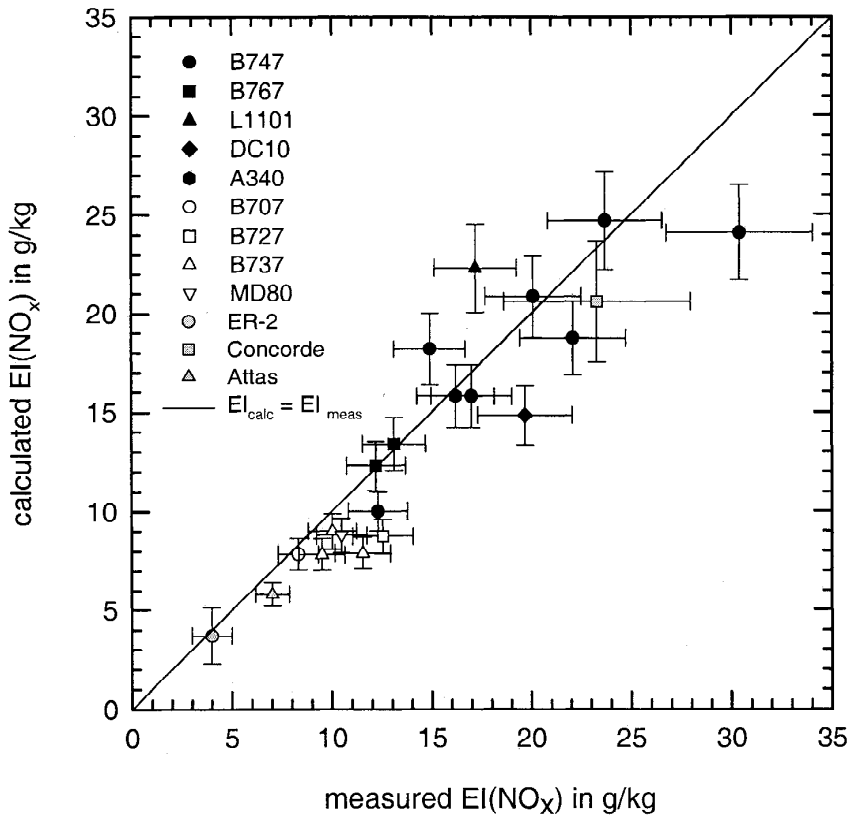

Figure 9. Measured versus computed emission indices EI(NO_x) (mass of NO_x in mass units of NO_2 per kg of burnt fuel) for various aircraft (as listed) under cruise conditions. Adapted from POLINAT 1 data and other data as described by *Schulte et al.* [1997], with additions from *Schlager et al.* [1997c], and as provided for *IPCC* [1999].

of 2 [*Schumann et al.*, 1998]. Figure 10 shows previous results together with the additional data points from POLINAT 2 listed in Table 9 (CO_2 and temperature measurements in the plume of the SONEX-DC-8 at 39630-39710 and 39950-40000 s UT October 23, 1997, and of the Airbus A340 on 25570 s UT September 24, 1997). The additional data are within the scatter of previous results.

4.4. Is There a Measurable Large-Scale Impact of Aircraft Emissions on the Composition of the Tropopause Region?

On the basis of the model results the mean relative contributions to NO_x concentration near the tropopause from aircraft in the POLINAT 2 region (see Plate 1) is higher than on average elsewhere in the northern midlatitudes [*Köhler et al.*, 1997]. Because of the large spatial and temporal variability and the peaky pattern of NO_x abundance in the corridors with many aircraft exhaust plumes, the experimental data provide a less obvious picture [*Schlager et al.*, 1997a, b].

A previous study performed within "Pollutants from Air Traffic" found large NO_y/O_3 ratios above the tropopause suggesting that air traffic emissions are an important NO_y source in the lowermost stratosphere [*Klemm et al.*, 1998]. This finding was confirmed within POLINAT 1 and 2 [*Ziereis et al.*, this issue].

POLINAT 1 provided the first measurements which indicate an impact of aircraft emissions on the NO_x concentration field at regional scales, at least under special weather conditions. The measurements within a stagnant anticyclone for 7 days in June 1995 show strong increases in NO_x, O_3, and particles. Model computations indicate that the observed NO_x increases can be explained (here on the basis of the CTM of KNMI) only when the aircraft emissions are included in the calculations, see Figure 11 [*Schlager et al.*, 1996].

The POLINAT 2 flights of September 21 and October 14 were specifically designed to measure in regions with predicted high impact of aircraft emissions to search for the corridor effect. These flights identified large-scale enhancements of the NO mixing ratio inside the corridor of about 50-150 pptv. These enhancements were attributed to aircraft emissions by correlations with simultaneous tracer measurements, back trajectory analyses, traffic distribution, and model predictions with and without aircraft emissions [*Schlager et al.*, 1999].

Some of the results presented in section 4.1 support the conclusion that aircraft cause enhanced NO_x and particle concentrations in the NAFC. This support comes in particular from the large local maximum values of NO_x, NO_y, and CN concentrations, and large NO_y/O_3 ratios, between 9.5 and 12 km altitude, see Figures 7 and 8. The maxima were found re-

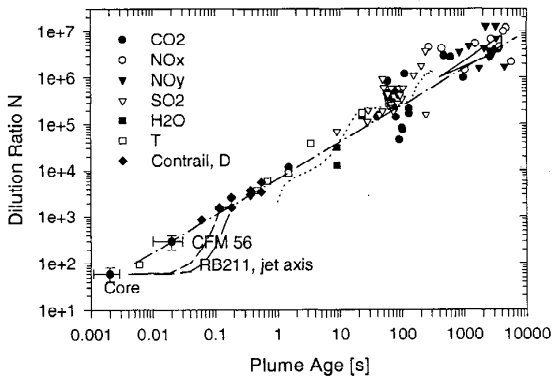

Figure 10. Dilution factor N (mass of air over which the exhaust from one unit mass of fuel burned got mixed per flight distance) versus plume age t. Adapted from *Schumann et al.* [1998] with additional data from temperature and CO_2 measurements in the exhaust plume of the SONEX DC-8 and the MOZAIC A340 for plume penetrations during POLINAT 2. The dotted line and the full-line triangle (at large plume ages) are numerical dilution results obtained by LES [*Gerz et al.*, 1998], the long-dashed curves at low plume ages represent dilution rates deduced from plume computations behind specific engines (CFM 56 and RB 211), and the dash-dotted line represents the approximation $N = 7000\ (t/t_0)^{0.8}$, $t_0 = 1$ s.

gardless of flying above or below the local tropopause and are not of stratospheric origin, therefore. The increases were observed in the NAFC between 50°-60°N, but not south of it. However, some of the local maxima occur in correlation with increases in SO_2 and CO, indicating contributions from surface sources. NO and NO_2 did not show a significant increase above the tropopause. This deviation from the expected C-shaped profile is more pronounced in NO than in NO_x values possibly because of faster oxidation of NO with O_3 above the tropopause [*Ziereis et al.*, this issue]. Also, some of the measured peaks may be due to still rather fresh aircraft emissions [*Schlager et al.*, 1997b].

The NO_x results obtained with the B-747 (see Plate 3) support an NO_x enhancement of the order of 50 pptv in the NAFC. *Brunner* [1998] identified that the short-term NO_x peaks caused by aircraft contribute about 20-30 pptv or 20-30% of the NO_x concentration measured along the routes across the North Atlantic of the B-747 during NOXAR.

The vertical CN profiles show a time-dependent enhancement of particulates within the corridor. Measurements within, above, and below the corridor revealed a nonvolatile aerosol enhancement of 3:1 at corridor altitudes [*Paladino et al.*, this issue].

As expected [*Schumann*, 1994], aircraft emissions in terms of CO_2, H_2O, CO, and SO_2 have small impact on the composition of the NAFC region and were not detectable in the measurements at corridor scales. Also, no corridor effect was found for acetone [*Arnold, et al.*, 1999]. Any corridor effect in HNO_3 if existing is within the scatter of the measurements [*Schlager et al.*, 1997b]. Hence regional aircraft-induced enhancements of air species in the corridor are measurable only for NO_x and particle number densities.

Table 9. Measured Plume Properties and Measured and Modeled Dilution Ratios N

Aircraft	Property	Age, s	Δ Property	N	$7000\ (t/1s)^{0.8}$
DC-8	CO_2	1.5±0.5	175 ppmv	11,800	9,700
DC-8	T	1.5±0.5	3.4 K	9,000	9,700
A340	CO_2	110±5	1.8 ppmv	1.2×10^6	0.3×10^6

4.5. What are the Contributions From Air Traffic Sources in Relation to Surface Emissions?

The models show that about 30 to 50% of the nitrogen oxides in the upper troposphere in the NAFC in autumn originates from aircraft emissions. Surface emissions contribute about the same magnitude to the NO_x abundance in the upper troposphere. Aircraft emissions predominate in the major air traffic regions over the United States of America, the North Atlantic, and Europe, with lightning sources providing the major input over subtropical and equatorial regions. While in the upper troposphere transport from the boundary layer besides aircraft emissions are the dominant sources, in the lower stratosphere this additional source is most likely air traffic [*Köhler et al.*, 1997, 1999; *Meijer et al.*, this issue; *Ziereis et al.*, this issue].

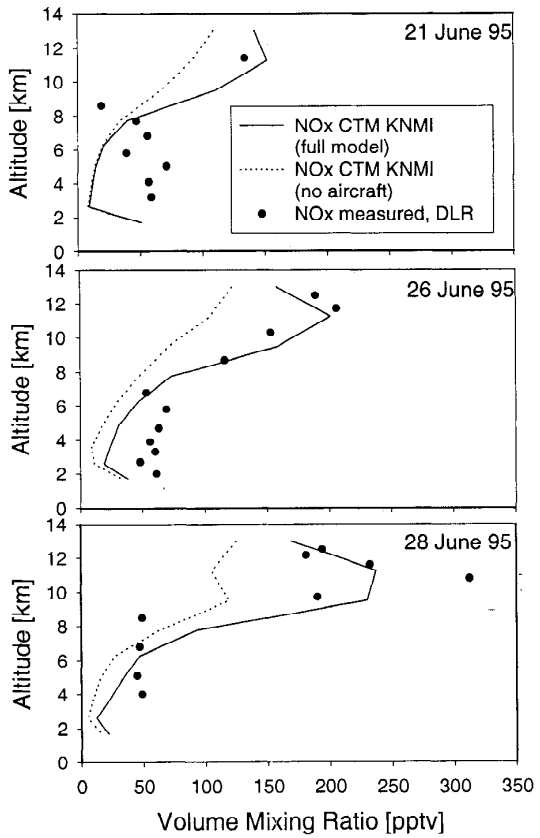

Figure 11. Mixing ratio of NO_x versus altitude as measured (symbols) and computed without (dotted curves) and with (solid curves) aircraft emissions during the period of a stagnant anticyclone over the British Islands in June 1995 [adapted from *Schlager et al.*, 1996].

During the POLINAT 1 project, clear indications for NO_x emissions from lightning were found during one flight at least (P6) [*Huntrieser et al.*, 1996]. On 5 days during the POLINAT 1 project, clear signals from surface emissions over the continental United States of America were found. These emissions could explain the high concentrations of SO_2, $(CH_3)_2CO$, and particles measured near the tropopause, see Figure 7, which cannot be caused by aircraft emission. By means of analyzed air trajectories it was shown that this pollution originated from surface emissions in the North American continent [e.g., *Arnold et al.*, 1997a]. During POLINAT 2, convective upward transport of subtropical marine boundary layer air (e.g., on September 21, 1997 [*van Velthoven*, 1999]) may explain the rather low O_3 values found near the tropopause (see Figure 7).

Surface emissions and lightning induced production of NO_x are clearly dominant in the upper troposphere in regions that are affected by convective events, in particular over the Gulf of Mexico [*Brunner et al.*, 1998]. In summer, the NO_x plumes are concentrated above the continental United States of America suggesting that lifting of air from the polluted continental boundary layer and/or lightning-produced NO_x lead to characteristic maximal mean concentration below the tropopause, see Plate 3. This is supported by the measurements in the month of August during POLINAT 2. Between September and November, the maximum NO_x concentration is found a few hundred kilometers offshore the east coast of the United States of America [*Jeker et al.*, this issue]. These results are consistent with the model predictions. For two cases of measurements with the B-747 in plumes of marine thunderstorms, where contribution from continental surface emissions are small, *Jeker et al.* [this issue] measured large NO concentrations in strong correlation with lightning events, suggesting that most of the plume NO originated from lightning.

4.6. How Frequent is Air at Flight Levels Supersaturated with Respect to the Ice Phase?

During the period of September to October 1997, the background levels of the relative humidity (RH) encountered during flights with the Falcon were generally very high. The humidity sometimes reached liquid saturation, see Figure 12, even at temperatures below -40°C. It has been confirmed that all the data shown were obtained with the hygrometer under conditions of stable loop control. Values exceeding liquid saturation by 5% could be explained by the error bar of the instrument. To prevent artifacts from rapid temperature changes, data with strong negative temperature changes were excluded, though this affected only a very small fraction of the data. The measured RH values reached up to 120% during the two flights F8 and F9 on the same day and in the same geographical area, during a short period of these flights. Such high values exceeding liquid saturation are presently not explainable. Supersaturation with respect to the ice phase, however, is to be expected if ice particles first nucleate via the liquid phase and then freeze. Ice nucleates from solution droplets near liquid saturation (100% RH) at temperatures above -39°C and at lower RH when the air is colder [*Heymsfield et al.*, 1998]. Even after ice formation the ice supersaturation may stay large because it takes time to diffuse the water vapor to the ice particles and because lifting of the air mass containing the particles may enhance the RH by adiabatic cooling.

The results show that the upper troposphere during summer and autumn 1997, and sometimes in November 1994 (but not in June/July 1995) was often supersaturated with respect to the ice phase. Persistent contrails were observed under such conditions. The data give no indication for a temperature-dependent RH-limit of ice nucleation as found by *Heymsfield et al.* [1998] in continental air masses. Marine air masses may behave differently because of different ice forming aerosol. Ice supersaturation was also found in the MOZAIC data [*Helten et al.*, 1999], and the data have implications for the amount of ice water content to be expected in contrails or cirrus clouds [*Schumann*, 2000].

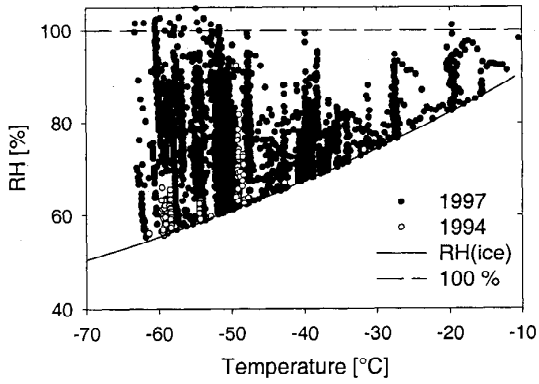

Figure 12. Relative humidity with respect to liquid water for cases exceeding ice saturation versus temperature. The plot shows all data measured outside young plumes excluding data during periods with temperature change less than -0.05 K/s. Data derived from the LMD frostpoint hygrometer and the DLR temperature sensors.

The humidity data are also used for determination of the threshold temperature T_c for contrail formation using the extended Schmidt-Appleman criterion as derived by *Schumann* [1996], see Table 8. The Schmidt-Appleman criterion predicts contrail formation when the plume humidity reaches liquid saturation at least locally. The data for cases 1 to 10, together with data from other recent measurements [*Schumann et al.*, 1996; *Jensen et al.*, 1998], have been already used by *Kärcher et al.* [1998] to test this criterion. Cases 11 and 12 provide further examples of contrails which are observed at ambient temperatures below the threshold temperatures T_c computed using this criterion. The threshold would be about 4 K higher than the value calculated if a contrail was formed when ice saturation was reached. For cases 2 and 5, no contrail formation was observed but contrails should have been visible if formed when the plume humidity locally exceeds ice saturation. Hence these cases provide further evidence that liquid saturation in the plume is necessary for contrail formation.

The extended Schmidt-Appleman criterion accounts for the so-called "η-effect" where η is the overall propulsion efficiency of the engine/aircraft combination [*Schumann*, 1996], that is, the fraction of combustion heat used to provide the work to propel the aircraft against its drag. Only the fraction $(1-\eta)$ of the heat but all of the H_2O from the fuel combustion leaves the engine with the exhaust gases. For larger values of η, the engine exhaust is cooler for the same water vapor concentration so that contrails form at higher ambient temperatures. For modern aircraft at cruise, η is typically between 0.3 and 0.36 [*Sausen et al.*, 1998]. Table 8 lists T_c computed for $\eta = 0.33$. The value of T_c for $\eta = 0.33$ is about 3.8 K higher than

for $\eta = 0$. For cases 4, 9, 10, and 12 the ambient temperature is below T_c computed for $\eta = 0.33$ but above T_c computed for $\eta = 0$. Contrails were observed for these cases. Hence these cases provide evidence that engines with high propulsion efficiency cause contrail formation at ambient temperature for which less efficient engines would cause no contrails.

Analyses of ECMWF data suggest that the upper troposphere in the main traffic region over the North Atlantic is conditioned to form persistent contrails about 15% of the time, with a seasonal maximum in October [*Sausen et al.*, 1998], which is in quantitative agreement with other observations [*Gierens et al.*, 1999; *IPCC*, 1999; *Schumann*, 2000].

4.7. How do the Instruments Perform in Flight in Comparison to Other Instruments?

Intercomparison flights of the Falcon with the Hercules C130 used in the ACSOE campaign, the Airbus A340 used in the MOZAIC project, the Swissair B-747, and the DC8 of SONEX have shown [*Ziereis et al.*, 1999b] that O_3 is measured with high accuracy (about 3% differences). For NO and NO_2, the data deviate typically by an order of 30% between various instruments, the best agreement (deviations <10%) was obtained for the Falcon/DC-8 intercomparison. The intercomparison is difficult because of the inhomogeneous NO_x field in the NAFC with large local concentration peaks from aged aircraft exhausts.

Data of the standard (PT500) temperature sensor on the Falcon and a temperature sensor on the C-130 where compared for nearly one hour (1310 - 1400 UTC) during the ACSOE/POLINAT 2 intercomparison flight F2 of September 21, 1997. The comparison reveals temperature differences of less than 0.1 K in the mean (less than 0.5 K in the signals) for temperatures between 255 and 260 K (with standard correction for the deicing heater). The MOZAIC-POLINAT intercomparisons gave a larger deviation (mean 0.64 K) between the two MOZAIC sensors and the standard PT500 sensor on the Falcon (possibly due to large deicing correction on the Falcon which flew at exceptionally large speed for this intercomparison), but better agreement of about 0.26 K when the MOZAIC data are compared to a second sensor on the Falcon (PT100, used for high-frequency measurements) [*Helten et al.*, 1999].

Water vapor measurements with the cryogenic frost-point hygrometer of LMD onboard the Falcon were compared in one case with those from a capacitive hygrometer onboard the MOZAIC-Airbus and were found to agree to better than 5% in mixing ratio for mixing ratios of 80 to 120 ppmv, and better than 15% in RH for RH between 40 and 80% of liquid saturation [*Helten et al.*, 1999]. The larger deviation of RH is a consequence of the bias between the Falcon and MOZAIC temperature measurements in this case. The RH values agree within 5% of liquid saturation when the temperature is computed from the PT100 instead of the PT500 temperature sensor on the Falcon.

The results of the LMD water vapor instrument were compared also with those of the laser diode instrument onboard the DC-8. The agreement between the two instruments is within the stated accuracy of the two instruments and is of about 10% in mixing ratio, in the range where the intercomparison occurred, from 100 to 900 ppmv [*Vay et al.*, this issue]. The laser diode instrument gives humidity mixing ratio values systematically higher than the one from the frost-point hygrometer. Hence the intercomparison supports the reliability of the high RH values found in POLINAT 2 (Figure 12). The correctly measured EI(H_2O) behind the DC-8 further supports the accuracy of the H_2O (and CO_2) instruments [*Ovarlez et al.*, this issue].

In several cases, the Falcon was flying a given track forward and backward, probing the same air masses twice within a short time period. These cases have been used to verify the reproducibility of the O_3, NO_x, HNO_3, SO_2, H_2O, wind, and temperature measurements. The results were always very satisfactory [*Schlager et al.*, 1997b; *Helten et al.*, 1999]. During ascents and descents, sometimes short periods of flights at constant flight level were introduced to check the temporal response of the instruments with respect to changes in the ambient conditions. These checks confirmed estimates of the response times of the instruments [e.g., *Ovarlez and van Velthoven*, 1997].

The first intercomparison of the only two acetone-detection methods presently used in the upper troposphere (CIMS of MPI-K during POLINAT 2 and a gas chromatographic technique of NASA-AMES during SONEX) shows agreement within the expected instrument accuracy of about ±30% [*Wohlfrom et al.*, 1999]. The intercomparison of POLINAT 2 data with the simultaneously registered SONEX data for SO_2 and HNO_3 revealed systematic discrepancies, which need further investigations [*Arnold et al.*, 1999].

Previous aerosol measurements of aerosol in the size range of 0.1 to 0.3 μm [*Konopka et al.*, 1997] are strongly affected by the large enrichment factor of the anisokinetic sampling device used, in particular when collecting aerosol contained in contrail or cirrus ice particles. As a consequence, analysis of the effective conversion fraction of fuel sulfur into sulfuric acid in the plume aerosol is not possible on the basis of the particle size spectra available up to now. Intercomparisons between UMR-MASS particle data and the particulate measurement instruments on the SONEX-DC-8 revealed agreement within the expected range of instrument accuracy [*Paladino et al.*, this issue].

4.8. How do the Models Perform in Comparison to Observations?

The POLINAT projects provide the opportunity for detailed case-by-case and statistical comparisons between measurements and models at the scales of individual single or multiple aircraft plumes, regional transverses across the corridor and vertical profiles near Ireland, and the whole east-west extent of the NAFC.

Comparisons to plume scale measurements [*Schumann et al.*, 1995; *Schlager et al.*, 1997a, b; *Dürbeck and Gerz*, 1996; *Gerz et al.*, 1998; *Schulte et al.*, 1997; *Tremmel et al.*, 1998; and *Kraabøl et al.*, 1999] used large-eddy simulations or considered plume dispersion by Gaussian models using anisotropic diffusivities and treat chemical conversion of NO_x to NO_y. The results are generally in good agreement with the observations.

At regional scales, the CTM results were evaluated along the tracks and vertical profiles taken by the Falcon, see, for example, Figure 13 [*Wauben et al.*, 1997b]. The agreement between modeled results and observations is reasonably good for O_3, but less clear for NO_x and systematically different for HNO_3. The models cannot resolve the peaky and patchy pattern of the NO_x concentration field measured at plume scales

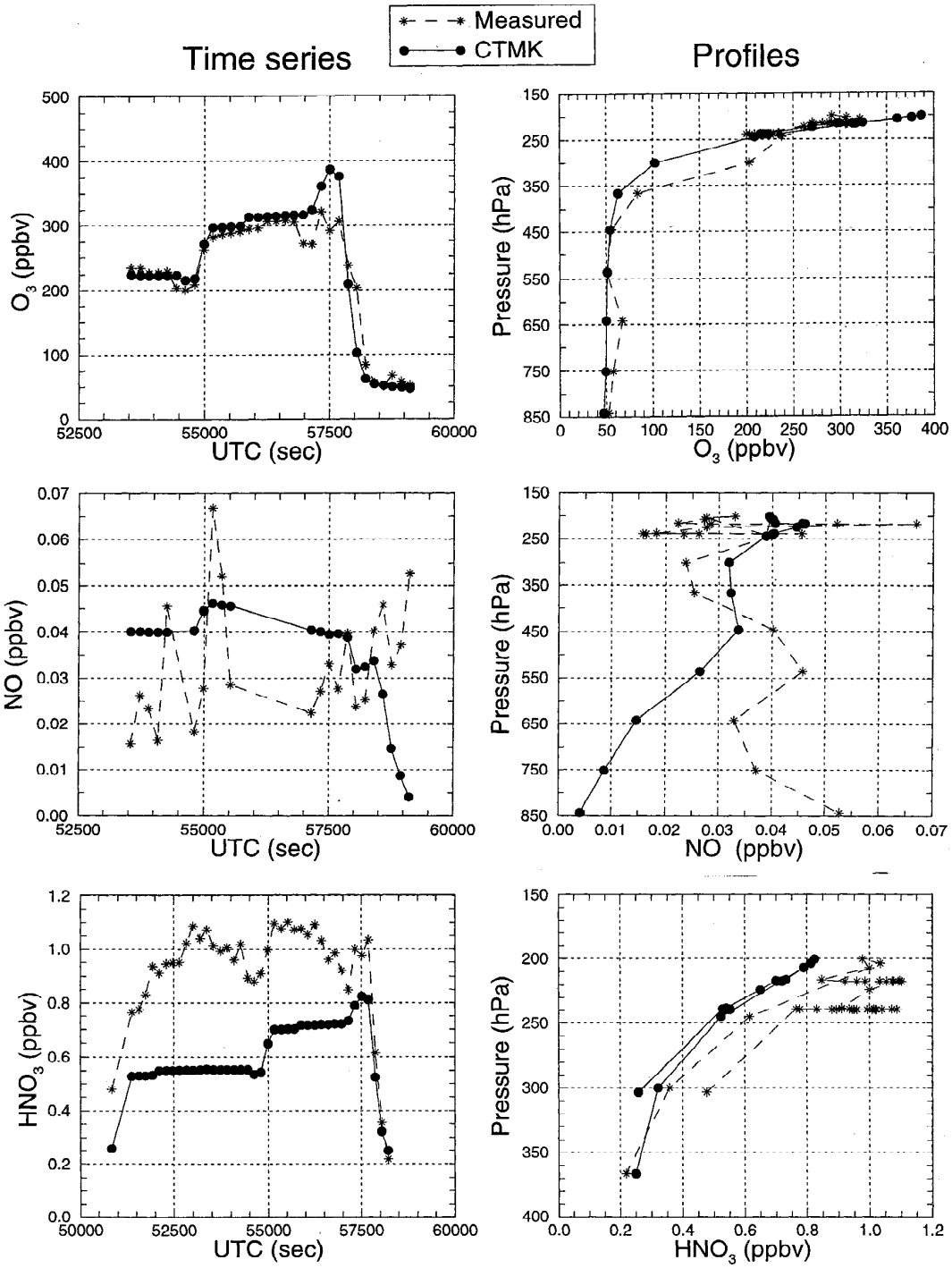

Figure 13. (left) Time series and (right) vertical profiles of measured (dashed curves with stars) and modeled (solid curves with dots, CTMK model) results of O_3, NO, and HNO_3 concentrations for November 2, 1994 [from *Wauben et al.*, 1997b].

and at the scales of convective events or within clouds. In view of the nonlinear dependence of O_3 formation rate on the NO_x concentration, these discrepancies are important and may cause an overestimate of the computed O_3 production rate by a factor of up to two [*Meijer et al.*, 1997; *Petry et al.*, 1998]. In Figure 13, the HNO_3 values modeled are below the measured values, and in other cases the opposite was found. This indicates possible uncertainties not only in the NO_x to NO_y conversion but also in the sinks of NO_y. Other studies report strong overpredictions of HNO_3 by models [*Hauglustaine et al.*, 1998; *Thakur et al.*, 1999], but our data provide higher HNO_3 levels which do not deviate systematically from the range expected from model predictions [*Schneider et al.*, 1998].

At the scale of the whole North Atlantic, the B-747 measurements performed within the NOXAR and POLINAT 2 projects provide the first possibility for simultaneous O_3 and NO_x model validations at such scales with a large data set. Plate 3 shows for example that the model ECHAM3/CHEM gives NO_x concentrations that agree with the measurements to within about 30% and shows very similar patterns in general, though details (e.g., ratio of NO_x maximum over mid-Europe relative to that at the East Coast of southern United States of America) differ [*Brunner*, 1998].

Global circulation model results can be compared to the statistics of the data measured during POLINAT and "Pollutants from Air Traffic" [*Schumann et al.*, 1997]. For example, Figure 14 shows the vertical profile of O_3 as computed with ECHAM3/CHEM in the model grid cell west of Ireland in comparison to the O_3 values measured with the Falcon in the same region in summer and autumn [*Köhler et al.*, 1999]. Apart from the values near the tropopause, which altitude is calculated to be too high in particular in the summer, the computed mean O_3 profiles are within the range of measured values, supporting the validity of this model. Similar comparison between ECHAM3/CHEM and measurements are shown for NO_x by *Ziereis et al.* [1999a]. Here the data agree within the range of one standard deviation of the model results at least in the upper troposphere and lower stratosphere. At low altitudes, the data show larger NO_x values than the model results.

Other models have difficulties in describing the dynamics of the tropopause regions also. For example, the maximum concentrations and the residence time of inert subsonic aircraft emissions near the tropopause have been found to vary by more than a factor of 2 between various models [*Danilin et al.*, 1998]. The results of global models are also highly sensitive to the modeling of convective transport. The global circulation model ECHAM3/NOX was run with and without subgrid-scale (SGS) models for convective transport of chemical constituents. The relevance of SGS convection was found to be more distinct in summer than in winter, as expected. When convection is switched off, only 12% of the original contribution (with convection) from NO_x surface emissions from the United States of America are found in the upper troposphere in the measurement area in June. For November, this number is 39%. On the other hand, the NO_x contribution from aircraft is almost independent of convection [*Köhler and Sausen*, 1997]. Washout in the troposphere is a further important process. Without wet removal, HNO_3 is lifted to the upper troposphere where it is photolyzed and acts as a source for NO_x. With wet removal of HNO_3 included, the sensitivity of NO_x and O_3 abundance to aircraft emissions is increased [*Jonson et al.*, 1999b].

The measured high acetone content above 1 ppbv, see Figure 7, from sources other than air traffic, is not yet fully reflected in the model studies. In summer, the large abundance of acetone provides a strong additional source for HO_x. Acetone may have a strong influence on the atmospheric oxidizing capacity and O_3 formation. This fact contributes to the uncertainty in present model results.

On the basis of the various studies and results, it can be expected that present models are able to predict increases of NO_x

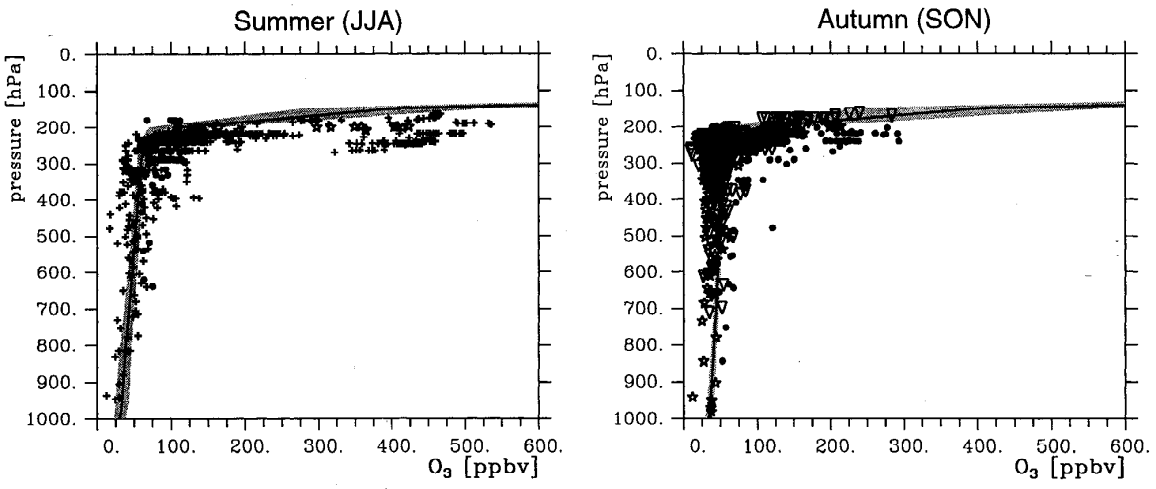

Figure 14. Comparison of measured O_3 mixing ratios (3 min averages; symbols) and the mean vertical profile of O_3 mixing ratio simulated with ECHAM3/CHEM (solid curve) and the standard deviation computed from 12 hourly computed data (shaded area) west of Ireland in (left) summer and (right) autumn. The different symbols indicate measurements from the different projects: full dots from POLINAT 1, triangles from POLINAT 2, and stars and crosses from "Pollutants from Air Traffic" 1994 and 1996, respectively [from *Köhler et al.*, 1999].

within the NAFC up to about an uncertainty factor of 2. The NO_x impact on O_3 occurs at larger scales after some downward, zonal, and meridional mixing, and depends on details of the HO_x chemistry, photolysis, and washout processes. The model uncertainty is estimated to be at least of the order of 2 on the basis of the scatter of results between various model approaches [*IPCC*, 1999].

4.9. What Are the Consequences of the Aircraft Emissions of Nitrogen Oxides and Other Trace Substances on the Formation of Ozone and Other Chemicals in the Troposphere and Lower Stratosphere?

The model calculations show that NO_x emissions from aircraft cause significant (about up to 25% in summer and 50% in autumn or winter) increase in the NO_x background concentrations in the NAFC, and the aircraft NO_x emissions cause increase in background O_3 concentrations by about 3-4% in winter and 5-6% in summer [e.g., *Köhler et al.*, 1999; *Meijer et al.*, this issue]. The emissions also cause an OH increase of up to 30% or more [*Hayman et al.*, 1999] and an HNO_3 increase of up to 10% in summer. The revised models [e.g., *Dameris et al.*, 1998; *Grewe et al.*, 1999] confirm earlier results that the present air traffic causes O_3 increases in the upper troposphere and in the lower stratosphere of about 4 to 8 ppbv in the region of the NAFC with background of 90-120 ppbv. The measured NO_x concentration is still low enough so that additional NO_x enhances O_3 production, in particular in air masses with high levels of acetone.

The relatively slow and small change in O_3 due to aircraft emissions in the NAFC could not be measured because of the large natural variability of O_3 near the tropopause. *Brunner et al.* [1998] find a positive correlation between enhanced upper tropospheric NO_x and O_3 but mainly because of NO_x from continental or lightning sources. A positive correlation between acetone and O_3 may be expected to exist in the troposphere because acetone contributes to HO_x and O_3 production at time scales similar to the residence time of acetone (order of 1 to 2 months). However, our data base indicates a weak correlation between the measured O_3 and acetone values.

4.10. What Can Be Learned About Atmospheric Dynamics From the Measurements and Model Results?

In view of the difficulty in modeling the tropopause altitude and the transport of aircraft emissions out of the tropopause region [*Danilin et al.*, 1998], studies of the tropopause dynamics are particularly needed. For many cases of tropopause transverses during POLINAT 1 and 2, the measured signals (O_3, H_2O, SO_2, HNO_3, wind speed, and wind-direction) often show nearly step-wise variations on short distances when the Falcon passed through the PV isosurface somewhere between 1.6 and 3.5 PVU [*Schumann*, 1997b; *Schlager et al.*, 1997b; *Ovarlez et al.*, 1999]. However, some tropopause traverses show a more complex picture indicating some cross-tropopause mixing. For example, flights N2, N3, and N4 (see Table 5) include observations within a developing tropopause fold, partly over-turning. A high potential vorticity (PV) "streamer" (up to 10 PVU) reaching from 70° to 30°N extending over about 10° west-east longitude, with near vertical tropopause between 500 and 220 hPa, was traversed on November 5 in east-west direction and again on November 6 in south-north direction. Figure 15 shows the PV isolines for the flight of November 5, from which one can identify the location of the tropopause. The figure also depicts the O_3 profiles measured at the corresponding flight altitudes versus longitudinal distance at nearly the same time. In this case, the O_3 tracer (and similarly the H_2O tracer, which is not plotted) increases nearly stepwise at about 8 km altitude at the plotted longitudinal distance of 270 km, but the PV contours indicate the tropopause to exist between 170 and 210 km distance in this plot. At other flight levels, the tracer tropopause is found also not to coincide with the dynamical tropopause in this case. Instead, the chemical tropopause lies higher than the thermal and dynamical ones, and the measured tracer profiles indicate a gradual change in O_3 and H_2O and not the expected stepwise increase near the dynamical tropopause. The NO and NO_2 data (not plotted) show also no clear transition from tropospheric to stratospheric values, and similar observations were made for some other cases [*Schlager et al.*, 1997a, b].

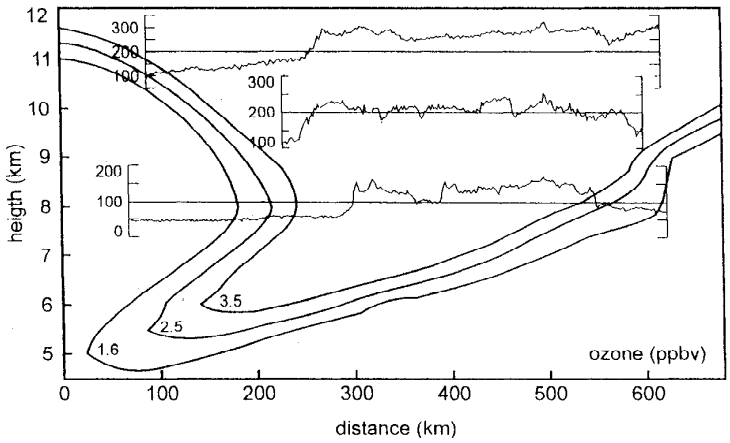

Figure 15. Isolines of potential vorticity (in PVU) in a vertical plane versus longitudinal distance (longitude increasing from left to right) and pressure altitude as derived from analyzed ECMWF data (T213/L31 resolution) for 1200 UT November 5, 1994, together with the altitudes of the flight segments at constant level (straight horizontal lines), and the ozone mixing ratio (in ppbv) measured at these positions between 0930 and 1220 UTC on the same day (flight N3) at about 52.5°N (provided by K. P. Hoinka).

Hence the observations indicate that some mixing occurs near such an overturning tropopause over vertical scales of order 5 km or over horizontal scales of about 50 to 100 km. The data offer an opportunity to investigate stratosphere-troposphere exchange including the transport of several trace constituents [*Ovarlez et al.*, 1999]. The Falcon crossed another tropopause fold on October 20, 1997 [*van Velthoven*, 1999] forming almost a cutoff low with aircraft emissions accumulating [*Meijer et al.*, this issue].

During flight N5 of November 8, 1994, wave fluctuations were observed in O_3 and H_2O concentrations and in the wind field. These fluctuations could be interpreted in terms of inertia-gravity waves. This fact is of importance for understanding small-scale transport processes [*Moustaoui et al.*, 1999].

The weather predictions provided by the ECMWF for planning the measurement program were found to be very reliable. In the case of the strong tropopause fold observed on November 5, 1994, the position of the fold was found to be within 50 km of the predicted position. Calculated temperatures were typically within 2-5 K of the measured values. Wind speed typically agrees within about 5-10 m s^{-1} [*van Velthoven*, 1999]. In the upper troposphere, when the water vapor concentration is below 20 ppmv, and in the lower stratosphere, calculated values are usually smaller than measured. This is caused by errors in the conventional radiosoundings and by the analysis scheme which assumed a very small background concentration of 5 ppmv in the lower stratosphere [*Ovarlez and van Velthoven*, 1997]. Recently, these findings have lead to changes in the ECMWF analysis scheme [*Simmons et al.*, 1999]. On the other hand, the ECMWF analysis assumes that humidity cannot exceed ice saturation, and hence underestimates the values under very humid conditions. Regions with measured ice supersaturation were found to coincide with ECMWF predictions of cirrus clouds [*Ovarlez et al.*, this issue].

5. Conclusions

During the POLINAT projects, measurements have been made of the composition of the atmosphere in the tropopause region in the altitude range from the midtroposphere to the lowermost stratosphere. The measurements cover the full altitude range and the horizontal range of cruising subsonic airliners in a vertical cross section perpendicular to the heavy air traffic in the NAFC. For NO_x and O_3 the measurements cover also the third dimension along the flight corridor between Europe and North America. In four series of experiments, eight measurement flights were performed in November 1994, nine in June/July 1995, seven in September 1997, and six in October 1997 with the Falcon, and about 100 measurements flights were performed from August to November 1997 with a B-747. Part of the measurements were performed in coordination with other experiments, in particular SONEX. Global and regional chemistry transport models were used to predict and analyze the contributions from aircraft emissions to the NO_x abundance and to O_3 formation. Also, the measurements were used to verify contrail formation criteria.

For the first time, the experiment showed that aircraft contribute measurable NO_x changes not only in plumes up to many hours but also at the scale of the whole corridor, at least under special meteorological conditions where aircraft emissions can accumulate during the period of a few days. However, at least equally often, high abundance of species were found that do not result from aircraft emissions but were transported from continental sources up into the upper troposphere. The background concentration of NO_x and other species were often found to be higher (up to 2.5 ppbv) than expected, with local maximum near the tropopause, suggesting contributions from aircraft. The models confirm earlier results that the present air traffic causes O_3 increases of a few percent in the upper troposphere and in the lower stratosphere. The calculated change in O_3 concentration is far more widespread than the change in nitrogen oxides and much smaller than its natural variability and hence could not be measured. It is found that acetone concentration is larger in the NAFC than over the Pacific. Acetone may enhance O_3 formation due to aircraft NO_x emissions. In the September/October season, very often ice supersaturated air masses were found with high supersaturation, sometimes reaching liquid saturation. The findings indicate a high potential for formation of persistent contrails in that period. Contrail formation and persistence was observed as expected from the revised Schmidt/Appleman criterion when accounting for engine efficiency.

In spite of the extensive measurement and modeling activities, several important questions remain open. In particular, no measurements have been performed under late winter conditions. At low ambient temperatures and high relative humidity at the tropopause, particle formation may occur with potentially important implications for chemistry, clouds, and climate. Data are missing also in summer over the European continent, where ozone precursors (acetone, other hydrocarbons, and carbon monoxide) may reach the upper troposphere by convective transport, and important amounts of lightning NO_x contributions are expected. The latter is the topic of the projects LINOX and EULINOX [*Huntrieser et al.*, 1998; *Höller et al.*, 1999] (http://www.pa.op.dlr.de/eulinox/). Except for lightning NO_x, the sources of the various species appear now to be known better than the sinks. Washout processes of nitric acid, for example, were shown to be important, but are still only crudely modeled and detailed measurements for model verification, in particular under cloudy conditions, are missing.

Finally, the models perform far from satisfactorily in describing the high spatial variability of short-lived species such as NO_x. Part of the model deficiencies are likely caused by the coarse numerical resolution affordable on present computers, but also deficiencies in modeling surface and lightning emissions, and transport and chemical aspects contribute to the observed differences. The models used are incomplete in describing the sources and sinks of acetone and its contribution to O_3 formation. This requires further model refinement. The data basis provided by the POLINAT projects is available for further studies of the atmospheric composition and its modeling.

Acknowledgments. We sincerely thank the European Commission (DG XII-D) for funding the POLINAT projects (contracts EV5V-CT93-0310 and ENV4-CT95-043), the Bundesministerium für Forschung und Technologie for funding work coordinated with POLINAT within the German project "Schadstoffe in der Luftfahrt", Swissair for providing the B-747 for measurements within POLINAT 2 and its predecessor NOXAR, and NASA for support of UMR and the cooperation of SONEX with POLINAT 2. The commitment and support by the DLR Flight Department is appreciated. We are also grateful to Shannon Air Traffic Control for their support and hospitality. We thank Swissair and Lufthansa for support in coordinating the intercomparison flights, and J. Vanier of ICAO Paris for providing data as used in Table 2 and Figure 1. Special appreciation is given to

Anne Thompson and Hanwant Singh (NASA-SONEX project scientists), and to the entire POLINAT and SONEX teams for the exciting and pleasant cooperation during the campaign. We gratefully acknowledge contributions from our coworkers who contributed as coauthors to various POLINAT reports and to the results presented in this paper in the various participating institutions: AEA: I. Ford (now at UCL), R. Kingdon (now at DERA Pyestock) , D. Lee (now at DERA Pyestock); DLR: T. Dürbeck (now with Siemens AG), C. Feigl, V. Grewe (presently at NASA-GISS), K.P. Hoinka, H. Huntrieser, I. Köhler, P. Konopka (now at Forschungszentrum Jülich), R. Sausen, P. Schulte, H.-G. Tremmel, H. Ziereis; ETH: D. Brunner, D. Jeker; FhG-IFU: O. Klemm (now at University of Bayreuth), F. Slemr; KNMI: E.W. Meijer, P.F.J. van Velthoven, W. Wauben; LMD: J. Capus, H. Ovarlez, R.-M. Philippe, H. Teitelbaum (also with KNMI); MPI-K: V. Bürger, B. Droste-Franke, T, Hauler, A. Jung, G. Kirchner, M. Klemm, B. Preissler, J. Schneider (now at Institut für Atmosphärenphysik, Kühlungsborn), K.-H. Wohlfrom; NILU: F. Flatøy, I. Fløisand, A. Kraabøl, F. Stordal; UO: J.E. Jonson, J. Sundet; UK Meteorological Office: C.E. Johnson, D.S. Stevenson; UMR: D.E. Hagen, A.R. Hopkins, J.D. Paladino, O. Schmidt, M.R. Wilson. In particular, we thank our colleagues for providing figures (as indicated in the figure captions).

References

Arnold, F., J. Scheid, and T. Stilp, H. Schlager, and M. E. Reinhardt, Measurements of jet aircraft emissions at cruise altitude, 1, The odd-nitrogen gases NO, NO_2, HNO_2, and HNO_3, *Geophys. Res. Lett., 19*, 2421-2424, 1992.

Arnold, F., J. Schneider, K. Gollinger, H. Schlager, P. Schulte, P. D. Whitefield, D. E. Hagen, and P. van Velthoven, Observation of upper tropospheric sulfur dioxide and acetone pollution: Potential implications for hydroxyl radical and aerosol formation, *Geophys. Res. Lett., 24*, 57-60, 1997a.

Arnold, F., V. Bürger, B. Droste-Franke, F. Grimm, A. Krieger, J. Schneider, and T. Stilp, Acetone in the upper troposphere and lower stratosphere: Impact on trace gases and aerosols, *Geophys. Res. Lett., 24*, 3017-3020, 1997b.

Arnold, F., K.-H. Wohlfrom, T. Hauler, M. Klemm, V. Bürger, B. Preissler, and A. Jung, Trace gas measurements by ion molecule reaction mass spectrometry during the POLINAT 2 campaign, in *POLINAT 2*, edited by U. Schumann, *EUR 18877 EN*, pp. 89-109, Eur. Comm., Luxembourg, 1999.

Baughcum, S. L., D. M. Chan, S. M. Happenny, S. C. Henderson, P. S. Hertel, T. Higman, D. R. Maggiora, and C. A. Oncina, Emissions scenarios development: Scheduled 1990 and projected 2015 subsonic, Mach 2.0 and Mach 2.4 aircraft, *NASA Publ. 1313*, pp. 87-131, 1993.

Berntsen, T., and I. S. A. Isaksen, A global 3-D chemical transport model for the troposphere, 1, Model description and CO and O_3 results, *J. Geophys. Res., 102*, 21,239-21,280, 1997.

Brasseur, G. P., J.-F. Müller, and C. Granier: Atmospheric impact of NO_x emissions by subsonic aircraft: A three-dimensional study, *J. Geophys. Res., 101*, 1423-1428, 1996.

Brasseur, G. P., R. A. Cox, D. Hauglustaine, I. Isaksen, J. Lelieveld, D. H. Lister, R. Sausen, U. Schumann, A. Wahner, and P. Wiesen, European scientific assessment of the atmospheric effects of aircraft emissions, *Atmos. Environ., 32*, 2327-2422, 1998.

Brunner, D., One-year climatology of nitrogen oxides and ozone in the tropopause region - results from B-747 aircraft measurements, Ph.D. thesis, Eidg. Tech. Hochsch. Zürich, 1998.

Brunner, D., J. Staehelin, and D. Jeker, Large-scale nitrogen oxide plumes in the tropopause region and implications for ozone, *Science, 282*, 1305-1309, 1998.

Campos, T. L., et al., Measurements of NO and NO_y emission indices during SUCCESS, *Geophys., Res. Lett., 25*, 1713-1716, 1998.

Curtius, J., B. Sierau, F. Arnold, R. Baumann, R. Busen, P. Schulte, and U. Schumann, First direct sulfuric acid detection in the exhaust plume of a jet aircraft in flight, *Geophys. Res. Lett., 25*, 923-926, 1998.

Dameris, M., V. Grewe, I. Köhler, R. Sausen, C. Brühl, J.-U. Grooß, and B. Steil: Impact of aircraft NO_x emissions on tropospheric and stratospheric ozone, part II, 3-D model results, *Atmos. Environ., 32*, 3185-3199, 1998.

Danilin, M. Y., et al., Aviation fuel tracer simulation: Model intercomparison and implications, *Geophys. Res. Lett., 25*, 3947-3950, 1998.

Dias-Lalcaca, P., D. Brunner, W. Imfeld, W. Moser, and J. Staehelin, An automated system for the measurements of nitrogen oxides and ozone concentrations from a passenger aircraft-instrumentation and first results of the NOXAR project, *Environ. Sci. Technol., 32*, 3228-3236, 1998.

Drummond, J. W., D. H. Ehhalt, and A. Volz, Measurements of nitric oxide between 0-12 km altitude and 67°N-60°S latitude obtained during STRATOZ III, *J. Geophys. Res., 93*, 15,831-15,849, 1988.

Dürbeck, T., and T. Gerz, Large-eddy simulation of aircraft exhaust plumes in the free atmosphere: Effective diffusivities and cross sections, *Geophys. Res. Lett., 22*, 3203-3206, 1995.

Dürbeck, T., and T. Gerz, Dispersion of aircraft exhausts in the free atmosphere, *J. Geophys. Res., 101*, 26,007-26,015, 1996.

Ehhalt, D. H., and F. Rohrer, The impact of commercial aircraft on tropospheric ozone, in *The Chemistry of the Atmosphere - Oxidants and Oxidation in the Earth's Atmosphere, 7th BOC Priestley Conference, Lewisburg, Pennsylvania*, edited by A. R. Brandy, *Spec. Publ. 170*, pp. 105-120, Roy. Soc. of Chem., London, 1994.

Ehhalt, D. H., F. Rohrer, and A. Wahner, Sources and distribution of NO_x in the upper troposphere at northern midlatitudes, *J. Geophys. Res., 97*, 3725-3738, 1992.

Emmons, L. K., et al., Climatologies of NO_x and NO_y: A comparison of data and models, *Atmos. Environ., 31*, 1851-1903, 1997.

Fahey, D. W., et al., Emission measurements of the Concorde supersonic aircraft in the lower stratosphere, *Science, 270*, 70-74, 1995.

Flatøy, F., and Ø. Hov, Three-dimensional model studies of the effect of NO_x emissions from aircraft on ozone in the upper troposphere over Europe and the North Atlantic, *J. Geophys. Res., 101*, 1401-1422, 1996.

Flatøy, F., and Ø. Hov, NO_x from lightning and the calculated chemical composition of the free troposphere, *J. Geophys. Res., 102*, 21,373-21,381, 1997.

Ford, I., An analytical model of the nucleation of a volatile aerosol in jet aircraft exhaust plumes, in *POLINAT 2*, edited by U. Schumann, *EUR 18877 EN*, pp. 249-268, Eur. Comm., Luxembourg, 1999a.

Ford, I., Ice nucleation in jet aircraft exhaust plumes, in *POLINAT 2*, edited by U. Schumann, *EUR 18877 EN*, pp. 269-287, Eur. Comm., Luxembourg, 1999b.

Ford, I., R. Kingdon, and G. Hayman, Numerical modeling of the optical properties of contrails, in *POLINAT 2*, edited by U. Schumann, *EUR 18877 EN*, pp. 233-248, Eur. Comm., Luxembourg, 1999.

Friedl, R. R. (Ed.), Atmospheric effects of subsonic aircraft: Interim assessment report of the advanced subsonic technology program, *NASA Ref. Publ., 1400*, 1997.

Fuelberg, H. E., J. R. Hannan, P. F. J. van Velthoven, E. V. Browell, G. Bieberbach Jr., R. D. Knabb, G. L. Gregory, K. E. Pickering, and H. B. Selkirk, A meteorological overview of the SONEX period, *J. Geophys. Res.*, this issue.

Fuglestvedt, J. S., I. S. A. Isaksen, and W.-C. Wang, Estimates of indirect global warming potentials for CH_4, CO and NO_x, *Clim. Change, 34*, 405-437, 1996.

Fuglestvedt, J. S., T. K. Berntsen, I. S. A. Isaksen, H. Mao, X.-Z. Liang, and W.-C. Wang, Climatic forcing of nitrogen oxides through changes in tropospheric ozone and methane; global 3-D model studies, *Atmos. Environ., 33*, 961-977, 1999.

Gardner, R.M. (Ed.), ANCAT/EC2 global aircraft emissions inventories for 1991/92 and 2015, Report by the ECAC/ANCAT and EC working group, *EUR 18179*, 84 pp., Eur. Comm. Dir. – Gen. XI, Brussels, 1998.

Gardner R., et al., The ANCAT/EC global inventory of NO_x emissions from aircraft, *Atmos. Environ., 31*, 1751-1766, 1997.

Gerbig, C., D. Kley, A. Volz-Thomas, J. Kent, K. Dewey, and D. S. McKenna, Fast response resonance fluorescence CO measurements aboard the C-130: Instrument characterization and measurements made during the North Atlantic Regional Experiment 1993, *J. Geophys. Res., 101*, 29,229-29,238, 1996

Gerz, T., T. Dürbeck, and P. Konopka, Transport and effective diffusion of aircraft emissions, *J. Geophys. Res., 103*, 25,905-25,913, 1998.

Gierens, K., U. Schumann, M. Helten, H. Smit, and A. Marenco, A distribution law for relative humidity in the upper troposphere and

lower stratosphere derived from three years of MOZAIC measurements, *Ann Geophys., 17,* 1218-1226, 1999.

Grewe, V., M. Dameris, R. Hein, I. Köhler, and R. Sausen, Impact of future subsonic aircraft NO_x emissions on the atmospheric composition, *Geophys. Res. Lett., 26,* 47-50, 1999.

Grooß, J.-U., C. Brühl, and T. Peter: Impact of aircraft emissions on tropospheric and stratospheric ozone, part I, Chemistry and 2-D model results, *Atmos. Environ., 32,* 3173-3184, 1998.

Hagen, D. E., P. D. Whitefield, and H. Schlager, Particulate emissions in the exhaust plume from commercial jet aircraft under cruise conditions, *J. Geophys. Res., 101,* 19,551-19,557, 1996.

Hauck, G., and F. Arnold, Improved positive-ion composition measurements in the upper troposphere and lower stratosphere and the detection of acetone, *Nature, 311,* 547-550, 1984.

Hauglustaine, D. A., C. Granier, G. P. Brasseur, and G. Mégie, Impact of present aircraft emissions of nitrogen oxides on tropospheric ozone and climate forcing, *Geophys. Res. Lett., 21,* 2031-2034, 1994.

Hauglustaine, D. A., G. P. Brasseur, S. Walters, P. J. Rasch, J.-F. Müller, L. K. Emmons, and M. A. Carroll, MOZART, a global chemical transport model for ozone and related chemical tracers, 2, Model results and evaluation, *J. Geophys. Res., 103,* 28,291-28,335, 1998.

Hayman, G. D., and M. Markiewicz, Chemical modeling of the aircraft exhaust plume, in *POLINAT,* edited by U. Schumann, *EUR 16978 EN,* pp. 280-303, Off. for Offi. Publ. of the Eur. Comm., Luxembourg, 1997.

Hayman, G., R. Kingdon, and D. Lee, Impact of different NO_x sources on ozone production in the upper troposphere, in *POLINAT 2,* edited by U. Schumann, *EUR 18877 EN,* pp. 191-215, Eur. Comm., Luxembourg, 1999.

Helten, M., H. G. J. Smit, W. Sträter, D. Kley, P. Nedelec, M. Zöger, and R. Busen, Calibration and performance of automatic compact instrumentation for the measurement of relative humidity from passenger aircraft, *J. Geophys. Res., 103,* 25,643-25,652, 1998.

Helten, M., H. G. J. Smit, D. Kley, J. Ovarlez, H. Schlager, R. Baumann, U. Schumann, P. Nedelec, and A. Marenco, In-flight intercomparison of MOZAIC and POLINAT water vapor measurements, *J. Geophys. Res.,* 104, 26,087-26,096, 1999.

Heymsfield, A. J., L. M. Miloshevich, C. Twohy, G. Sachse, and S. Oltmans, Upper tropospheric relative humidity observations and implications for cirrus ice nucleation, *Geophys. Res. Lett., 25,* 1343-1346, 1998.

Hoinka, K. P., Statistics of the global tropopause pressure, *Mon. Weather Rev., 126,* 3303-3325, 1998.

Hoinka, K. P., M.E. Reinhardt, and W. Metz, North Atlantic air traffic within the lower stratosphere: Cruising times and corresponding emissions, *J. Geophys. Res., 98,* 23,113-23,131, 1993.

Höller, H., U. Finke, H. Huntrieser, M. Hagen, and C. Feigl, Lightning-produced NO_x (LINOX): Experimental design and case study results, *J. Geophys. Res., 104,* 13,911-13,922, 1999.

Hov, Ø., and F. Flatøy, Convective redistribution of ozone and oxides of nitrogen in the troposphere over Europe in summer and fall, *J. Atmos. Chem., 28,* 319-337, 1997.

Huntrieser, H., H. Schlager, P. van Velthoven, P. Schulte, H. Ziereis, U. Schumann, F. Arnold, and J. Ovarlez, In-situ trace gas observations in dissipating thunderclouds during POLINAT, in *Proceedings of the 12th International Conference on Clouds and Precipitation,* pp. 1058-1061, Zürich, Am. Meteorol. Soc., Boston, Mass., 1996.

Huntrieser, H., H. Schlager, C. Feigl, and H. Höller, Transport and production of NO_x in electrified thunderstorms: Survey of previous studies and new observations at midlatitudes, *J. Geophys. Res., 103,* 28,247-28,264, 1998.

International Civil Aviation Organization (ICAO), North Atlantic air traffic forecasts for the years 1997-2002, 2005, 2010 and 2015, 68 pp., North Atl. Traffic Forecasting Group, Europ. and North Atl. Off., Paris, 1997.

Intergovernmental Panel on Climate Change (IPCC), *Aviation and the Global Atmosphere,* edited by J. E. Penner et al., Cambridge Univ. Press, New York, 1999.

Isaksen, I., and C. Jackman, Modeling the chemical composition of the future atmosphere, in *Aviation and the Global Atmosphere, IPCC Special Report,* pp. 121-163, Cambridge Univ. Press, New York, 1999.

Jeker, D. P., et al., Measurements of nitrogen oxides at the tropopause: Attribution to convection and correlation with lightning, *J. Geophys. Res.,* this issue.

Jensen, E. J., O. B. Toon, S. Kinne, G. W. Sachse, B. E. Anderson, K. R. Chan, C. H. Twohy, B. Gandrud, A. Heymsfield, and R. C. Miake-Lye, Environmental conditions required for contrail formation and persistence, *J. Geophys. Res., 103,* 3929-3936, 1998.

Jonson, J. E., L. Tarrason, and J. Sundet, Calculation of ozone and other pollutants for the summer 1996, *Environ. Manage. Health, 10,* 245-257, 1999a.

Jonson, J. E., I. S. A. Isaksen, and J. Sundet, Calculated effects of aircraft emissions in the North Atlantic flight corridor, in *POLINAT 2,* edited by U. Schumann, *EUR 18877 EN,* pp. 177-190, Luxembourg, Eur. Comm., 1999b.

Kärcher, B., R. Busen, A. Petzold, F. P. Schröder, U. Schumann, and E. J. Jensen, Physicochemistry of aircraft-generated liquid aerosols, soot, and ice particles, 2, Comparison with observations and sensitivity studies, *J. Geophys. Res., 103,* 17,129-17,147, 1998.

Ker, A., North Atlantic air traffic report 1997: Air statistics and forecasts, 24 pp., Econ. Anal., Transp. Can., Ottawa, Ontario, 1998.

Klemm, O., W. R. Stockwell, H. Schlager, and H. Ziereis, Measurements of nitrogen oxides from aircraft in the northeast Atlantic flight corridor, *J. Geophys. Res., 103,* 31,217-31,230, 1998.

Köhler, I., and R. Sausen, Contributions of various NO_x sources to the atmospheric NO_x content in the POLINAT region, in *POLINAT,* edited by U. Schumann, *EUR 16978 EN,* pp. 139-147, Eur. Comm., Luxembourg, 1997.

Köhler, I., R. Sausen, and R. Reinberger, Contributions of aircraft emissions to the atmospheric NO_x content, *Atmos. Environ., 31,* 1801-1818, 1997.

Köhler, I., R. Sausen, V. Grewe, and H. Ziereis, Intercomparison of global model simulations and aircraft measurements in the NAFC, in *POLINAT 2,* edited by U. Schumann, *EUR 18877 EN,* pp. 217-232, Luxembourg, Eur. Comm., 1999.

Konopka, P., U. Schumann, H. Schlager, D. E. Hagen, P. D. Whitefield, and J. Ovarlez, Particulate emissions of commercial jet aircraft under cruise conditions, Rep. 93, 13 pp., Inst. Phys. Atmos., DLR Oberpfaffenhofen, Germany, 1997.

Kraabøl, A. G., F. Stordal, I. Ford, and I. Fløisand, Particles and heterogeneous chemistry in aircraft plumes, in *POLINAT 2,* edited by U. Schumann, *EUR 18877 EN,* pp. 289-306, Eur. Comm., Luxembourg, 1999.

Kraus, A. B., F. Rohrer, E. S. Grobler, and D. H. Ehhalt, The global tropospheric distribution of NO_x estimated by a 3-D chemical tracer model, *J. Geophys. Res., 101,* 18,587-18,604, 1996.

Lee, D. S., I. Köhler, E. Grobler, F. Rohrer, R. Sausen, L. Gallardo-Klenner, J. J. G. Olivier, F. J. Dentener, and A. F. Bouwman, Estimates of global NO_x emissions and their uncertainties, *Atmos. Environ., 31,* 1735-1749, 1997.

Marenco A., et al., Measurement of ozone and water vapor by Airbus in-service aircraft: The MOZAIC airborne program, an overview, *J. Geophys. Res., 103,* 25,631-25,642, 1998.

Meijer, E. W., P. J. F. van Velthoven, W. M. F. Wauben, H. Kelder, J. P. Beck, and G. J. M. Velders, The effect of the conversion of nitrogen oxides in aircraft exhaust plumes in global models, *Geophys. Res. Lett., 24,* 3013-3016, 1997.

Meijer, E. W., P. J. F. van Velthoven, A. M. Thompson, L. Pfister, H. Schlager, P. Schulte, and H. Kelder, Model calculations of the impact of NO_x from air traffic, lightning, and surface emissions, compared with measurements, *J. Geophys. Res.,* this issue.

Moustaoui, M., H. Teitelbaum, P. F. J. van Velthoven, and H. Kelder, Analysis of gravity waves during the POLINAT experiment and some consequences for stratosphere-troposphere exchange, *J. Atmos. Sci., 56,* 1019-1030, 1999.

Müller, J.-F., and G. Brasseur, Sources of upper tropospheric HO_x: A three-dimensional study, *J. Geophys. Res., 104,* 1705-1715, 1999.

Ovarlez, J., and P. van Velthoven, Comparison of water vapor measurements with data retrieved from ECMWF analysis during the POLINAT experiment, *J. Appl. Meteorol., 36,* 1329-1335, 1997.

Ovarlez, J., P. F. J. van Velthoven, and H. Schlager, Water vapor measurements from the troposphere to the lowermost stratosphere: Some signatures of troposphere to stratosphere exchanges, *J. Geophys. Res.,* 104, 16,973-16,978, 1999.

Ovarlez, J., P. van Velthoven, G. Sachse, S. Vay, H. Schlager, and H. Ovarlez, Comparison of water vapor measurements from POLINAT 2 with ECMWF analyses in high-humidity conditions, *J. Geophys. Res.,* this issue.

Paladino, J., P. Whitefield, D. Hagen, A. R. Hopkins, and M. Trueblood, Particle concentrations characterization for jet engine emissions under cruise conditions, *Geophys. Res. Lett., 25*, 1697-1700, 1998.

Paladino, J. D., D. E. Hagen, P. D. Whitefield, A. R. Hopkins, O. Schmidt, M. R. Wilson, and H. Schlager, Observations of particulates within the North Atlantic flight corridor: POLINAT 2, September – October 1997, *J. Geophys. Res.*, this issue.

Penner, J.E., C. S. Atherton, J. Dignon, S. J. Ghan, and J. J. Walton, Tropospheric nitrogen: A three-dimensional study of sources, distributions, and deposition, *J. Geophys. Res., 96*, 959-990, 1991.

Petry, H., J. Hendricks, M. Möllhoff, E. Liepert, A. Meier, A. Ebel, and R. Sausen, Chemical conversion of subsonic aircraft emissions in the dispersing plume: Calculation of effective emission indices, *J. Geophys. Res., 103*, 5759-5772, 1998.

Ponater, M., S. Brinkop, R. Sausen, and U. Schumann, Simulating the global atmospheric response to aircraft water vapour emissions and contrails: A first approach using a GCM, *Ann. Geophys., 14*, 941-960, 1996.

Rohrer, F., D. Brüning, and D. H. Ehhalt, Tropospheric mixing ratios of NO obtained during TROPOZ II in the latitude region 67°N-56°S, *J. Geophys. Res., 102*, 25,429-25,449, 1997a.

Rohrer, F., et al., On the increase of NO_x and NMHC mixing ratios in the upper troposphere due to aircraft emissions, in *Pollutants from Air Traffic - Results of Atmospheric Research 1992-1997*, edited by U. Schumann et al., *DLR-Mitt. 97-04*, pp. 271-279, DLR, Köln, Germany, 1997b.

Sausen, R., B. Feneberg, and M. Ponater, Climatic impact of aircraft induced ozone changes, *Geophys. Res. Lett., 24*, 1203-1206, 1997.

Sausen, R., K. Gierens, M. Ponater, and U. Schumann, A diagnostic study of the global coverage by contrails, part I, Present day climate, *Theor. Appl. Climatol., 61*, 127-141, 1998.

Schlager, H., P. Schulte, H. Ziereis, F. Arnold, J. Ovarlez, P. van Velthoven, and U. Schumann, Airborne observations of large-scale accumulations of air traffic emissions in the North Atlantic flight corridor within a stagnant anticyclone, in *Proceedings International Colloquium Impact of Aircraft Emissions Upon the Atmosphere, 1*, pp. 247-252, Off. Natl. d'Etudes et de Rech. Aerosp., Chatillon, Paris, October 15-18, 1996.

Schlager, H., P. Schulte, H. Ziereis, P. Konopka, U. Schumann, C. Feigl, R. Marquardt, and H. Huntrieser, Aircraft-borne measurements of NO_x, O_3, and CO_2, in *POLINAT*, edited by U. Schumann, *EUR 16978 EN*, pp. 20-47, Off. for Offi. Publ. of the Eur. Comm., Luxembourg, 1997a.

Schlager, H., P. Konopka, P. Schulte, U. Schumann, H. Ziereis, F. Arnold, M. Klemm, D. E. Hagen, P.D. Whitefield, and J. Ovarlez, In situ observations of air traffic emission signatures in the North Atlantic flight corridor, *J. Geophys. Res., 102*, 10,739-10,750, 1997b.

Schlager, H., P. Schulte, and H. Ziereis, In-situ measurements in aircraft exhaust plumes and in the North Atlantic flight corridor, edited by U. Schumann, *DLR-Mitt. 97-04*, pp. 57-66, DLR, Köln, Germany, 1997c.

Schlager, H., P. Schulte, F. Flatøy, F. Slemr, P. van Velthoven, H. Ziereis, and U. Schumann, Regional nitric oxides enhancements in the North Atlantic flight corridor observed and modeled during POLINAT 2, a case study, *Geophys. Res. Lett., 26*, 3061-3064.

Schneider, J., et al., Nitric acid (HNO_3) in the upper troposphere and lower stratosphere at midlatitudes: New results from aircraft-based mass spectrometric measurements, *J. Geophys. Res., 103*, 25,337-25,343, 1998.

Schröder, F. P., B. Kärcher, A. Petzold, R. Baumann, R. Busen, C. Hoell, and U. Schumann, Ultrafine aerosol particles in aircraft plumes: In situ observations, *Geophys. Res. Lett., 25*, 2789-2792, 1998.

Schulte, P., and H. Schlager, In-flight measurements of cruise altitude nitric oxide emission indices of commercial jet aircraft, *Geophys. Res. Lett., 23*, 165-168, 1996.

Schulte, P., H. Schlager, H. Ziereis, U. Schumann, S. L. Baughcum, and F. Deidewig, NO_x emission indices of subsonic long-range jet aircraft at cruise altitude: In situ measurements and predictions, *J. Geophys. Res., 102*, 21,431-21,442, 1997.

Schumann, U., On the effect of emissions from aircraft engines on the state of the atmosphere, *Ann. Geophys., 12*, 365-384, 1994.

Schumann, U. (Ed.), AERONOX — The impact of NO_x emissions from aircraft upon the atmosphere at flight altitudes 8-15 km, *Publ. EUR 16209 EN*, 471 pp., Off. for Publ. of the Eur. Comm., Brussels, 1995.

Schumann, U., On conditions for contrail formation from aircraft exhausts, *Meteorol. Z., 5*, 4-24, 1996.

Schumann, U., The impact of nitrogen oxides emissions from aircraft upon the atmosphere at flight altitudes — Results from the AERONOX project, *Atmos. Environ., 31*, 1723-1733, 1997a.

Schumann, U. (Ed.), Pollution From Aircraft Emissions in the North Atlantic Flight Corridor (POLINAT), Air pollution research rep. 58, *Rep. EUR 16978 EN*, 303 pp., Off. for Offi. Publ. of the Eur. Communities, Luxembourg, 1997b.

Schumann, U. (Ed.), Pollution from Aircraft Emissions in the North Atlantic Flight Corridor (POLINAT 2), Air pollution research report, *Rep. EUR 18877 EN*, 308 pp., Off. for Offi. Publ. of the Eur. Communities, Luxembourg, 1999.

Schumann, U., Contrail cirrus, in *Cirrus*, edited by D. Lynch, Oxford Univ. Press, New York, in press, 2000.

Schumann, U., and P. Konopka, A simple estimate of the concentration field in a flight corridor, in *Impact of Emissions From Aircraft and Spacecraft Upon the Atmosphere*, edited by U. Schumann and D. Wurzel, *DLR-Mitt. 94-06*, pp. 354-359, DLR, Köln, Germany, 1994.

Schumann, U., P. Konopka, R. Baumann, R. Busen, T. Gerz, H. Schlager, P. Schulte, and H. Volkert, Estimate of diffusion parameters of aircraft exhaust plumes near the tropopause from nitric oxide and turbulence measurements, *J. Geophys. Res., 100*, 14,147-14,162, 1995.

Schumann, U., J. Ström, R. Busen, R. Baumann, K. Gierens, M. Krautstrunk, F.P. Schröder, and J. Stingl, In situ observations of particles in jet aircraft exhausts and contrails for different sulfur containing fuels, *J. Geophys. Res., 101*, 6853-6869, 1996.

Schumann, U., A. Chlond, A. Ebel, B. Kärcher, H. Pak, H. Schlager, A. Schmitt, and P. Wendling (Eds.), Pollutants from air traffic - Results of atmospheric research 1992-1997, *DLR-Mitt. 97-04*, 291 pp., DLR, Köln, Germany, 1997.

Schumann U., H. Schlager, F. Arnold, R. Baumann, O. Haschberger, and O. Klemm, Dilution of aircraft exhaust plumes at cruise altitudes, *Atmos. Environ., 32*, 3097-3104, 1998.

Simmons, A. J., A. Untch, C. Jakob, P. Kållberg, and P. Undén, Stratospheric water vapor and tropical tropopause temperature in ECMWF analyses and multi-year simulations. *Q. J. R. Meteorol. Soc., 125*, 353-386, 1999.

Singh, H. B., M. Kanakidou, P. J. Crutzen, and D. J. Jacob, High concentrations and photochemical fate of oxygenated hydrocarbons in the global troposphere, *Nature, 378*, 50-54, 1995.

Singh, H. B., et al., Latitudinal distribution of reactive nitrogen in the free troposphere over the Pacific Ocean in late winter/early spring, *J. Geophys. Res., 103*, 28,237-28,246, 1998.

Singh, H. B., A. M. Thompson, and H. Schlager, SONEX airborne mission and coordinated POLINAT 2 activity: Overview and accomplishments, *Geophys. Res. Lett., 26*, 3053-3056.

Slemr, F., H. Giehl, J. Slemr, R. Busen, P. Haschberger, and P. Schulte, In-flight measurements of aircraft nonmethane hydrocarbon emission indices, *Geophys. Res. Lett., 25*, 321-324, 1998.

Steil, B., M. Dameris, C. Brühl, P.J. Crutzen, V. Grewe, M. Ponater, and R. Sausen, Development of a chemistry module for GCMS - First results of a multiannual integration, *Ann. Geophys., 16*, 205-228, 1998.

Stevenson, D. S., W. J. Collins, C. E. Johnson, and R. G. Derwent, The impact of aircraft nitrogen oxide emissions on tropospheric ozone studied with a 3-D Lagrangian model including fully diurnal chemistry, *Atmos. Environ., 31*, 1837-1850, 1997.

Thakur, A. N., H. B. Singh, P. Mariani, Y. Chen, Y. Wang, D. J. Jacob, G. Brasseur, J.-F. Müller, and M. Lawrence, Distribution of reactive nitrogen species in the remote free troposphere: Data and model comparisons, *Atmos. Environ., 33*, 1403-1422, 1999.

Tremmel, H. G., H. Schlager, P. Konopka, P. Schulte, F. Arnold, M. Klemm, and B. Droste-Franke, Observations and model calculations of jet aircraft exhaust products and cruise altitude and inferred initial OH emissions, *J. Geophys. Res., 103*, 10,803-10,816, 1998.

van Velthoven, P., Meteorological support for the POLINAT 2 flights, in *POLINAT 2*, edited by U. Schumann, *EUR 18877 EN*, pp. 139-147, Eur. Comm., Luxembourg, 1999.

van Velthoven, P. F. J., et al., The passive transport of NO_x emissions

from aircraft studied with a hierarchy of models, *Atmos. Environ., 31*, 1783-1799, 1997.

Vay, S. A., B. E. Anderson, E. J. Jensen, G. W. Sachse, J. Ovarlez, G. L. Gregory, S. R. Nolf, J. R. Poldoske, T. A. Slate and C. E. Sorenson, Tropospheric water vapor measurements over the North Atlantic during SONEX, *J. Geophys. Res.*, this issue.

Wauben, W. M. F., P. F. J. van Velthoven, and H. Kelder, A 3-D chemical transport model study of changes in atmospheric ozone due to aircraft emissions, *Atmos. Environ., 31*, 1819-1736, 1997a.

Wauben, W. M. F., P. F. J. van Velthoven, and H. Kelder, The impact of air traffic in the NAFC: Model results and measurements, in *POLINAT*, edited by U. Schumann, *EUR 16978 EN*, pp. 122-133, Off. for Offi. Publ. of the Eur. Comm., Luxembourg, 1997b.

Weinheimer, A.J., J. G. Walega, B. A. Ridley, B. L. Gary, D. R. Blake, N. J. Blake, F. S. Rowland, G. W. Sachse, B. E. Anderson, and J. E. Collins, Meridional distributions of NO_x, NO_y, and other species in the lower stratosphere and upper troposphere during AASE II, *Geophys. Res. Lett., 21*, 2583-2586, 1994.

Wennberg, P. O., et al., Hydrogen radicals, nitrogen radicals and the production of ozone in the upper troposphere, *Science, 279*, 49-53, 1998.

Wohlfrom, K.-H., T. Hauler, F. Arnold, and H. Singh, Acetone in the free troposphere and lower stratosphere: Aircraft-based CIMS and GC measurements over the North Atlantic and a first comparison, *Geophys. Res. Lett., 26*, 2849-2852, 1999.

World Meteorological Organization (WMO), Scientific assessment of ozone depletion: 1994, Geneva, 1995.

Ziereis, H., H. Schlager, P. Schulte, I. Köhler, R. Marquardt, and C. Feigl, In situ measurements of the NO_x distribution and variability over the eastern North Atlantic, *J. Geophys. Res., 104*, 16,021-16,032, 1999a.

Ziereis, H., H. Schlager, and P. Schulte, NO, NO_y, and O_3 intercomparisons during POLINAT 2, in *POLINAT 2*, edited by U. Schumann, *EUR 18877 EN*, pp. 55-63, Eur. Comm., Luxembourg, 1999b.

Ziereis, H., H. Schlager, P. Schulte, P.F.J. van Velthoven, and F. Slemr, Distributions of NO, NO_x, and NO_y in the upper troposphere and lower stratosphere between 28°N and 61°N during POLINAT 2, *J. Geophys. Res.*, this issue.

F. Arnold, Bereich Atmosphärenphysik, MPI für Kernphysik, Postfach 103980, 69117 Heidelberg, Germany. (Frank.Arnold@mpi-hd.mpg.de)

G. Hayman, AEA Technology, National Environmental Technology Centre, E5 Culham, Abingdon, Oxon. OX14 3ED, England, U.K. (Garry.Hayman@aeat.co.uk)

Ø. Hov, NILU, P.O. Box 64, 2001 Lillestrom, Norway. (Oystein.Hov@nilu.no)

I.S.A. Isaksen, Department of Geophysics, University of Oslo, Oslo, BP 1022, Blindern, 0315 Oslo 5, Norway. (Ivar.Isaksen@geofysikk.uio.no)

H. Kelder, KNMI, Postbus 201, 3730 AE de Bilt, Netherlands. (Kelder@knmi.nl)

J. Ovarlez, LMD du CNRS, Palaiseau, 91128 Palaiseau Cedex, France. (joelle.ovarlez@polytechnique.fr)

H. Schlager and U. Schumann (corresponding author), Institut für Physik der Atmosphäre, DLR, Postfach 1116, 82230 Wessling, Germany. (Hans.Schlager@dlr.de; Ulrich.Schumann@dlr.de)

J. Staehelin, Institute for Atmospheric Science, ETH, Hönggerberg HPP, 8093 Zürich, Switzerland. (Staehelin@atmos.umnw.ethz.ch)

P.D. Whitefield, Laboratory for Cloud and Aerosol Science, University of Missouri-Rolla, G-7 Norwood Hall, Rolla, MO 65401. (pwhite@physics.umr.edu)

(Received April 12, 1999; revised September 1, 1999;
accepted September 6, 1999)